# Precision Stellar Photometry and Astrometry using Discrete Point Spread Functions: Theory and Practice

Kenneth John Mighell

National Optical Astronomy Observatory


*NESSI/CTI-II Team Meeting* December 1-2, 2006

Department of Physics and Astronomy, University of New Mexico, Albuquerque

This work is supported by a grant, Interagency Order No. NNG06EC81I, from the **Applied Information Systems Research (AISR)** Program of the Science Mission Directorate of the National Aeronautics and Space Administration (NASA).

# Outline

- Introduction
- Point Response Functions
- Performance Model based on Information Theory
- Photometry and Astrometry with Discrete PSFs
- Spitzer Space Telescope's Infrared Array Camera

# Introduction

# Image Formation Process

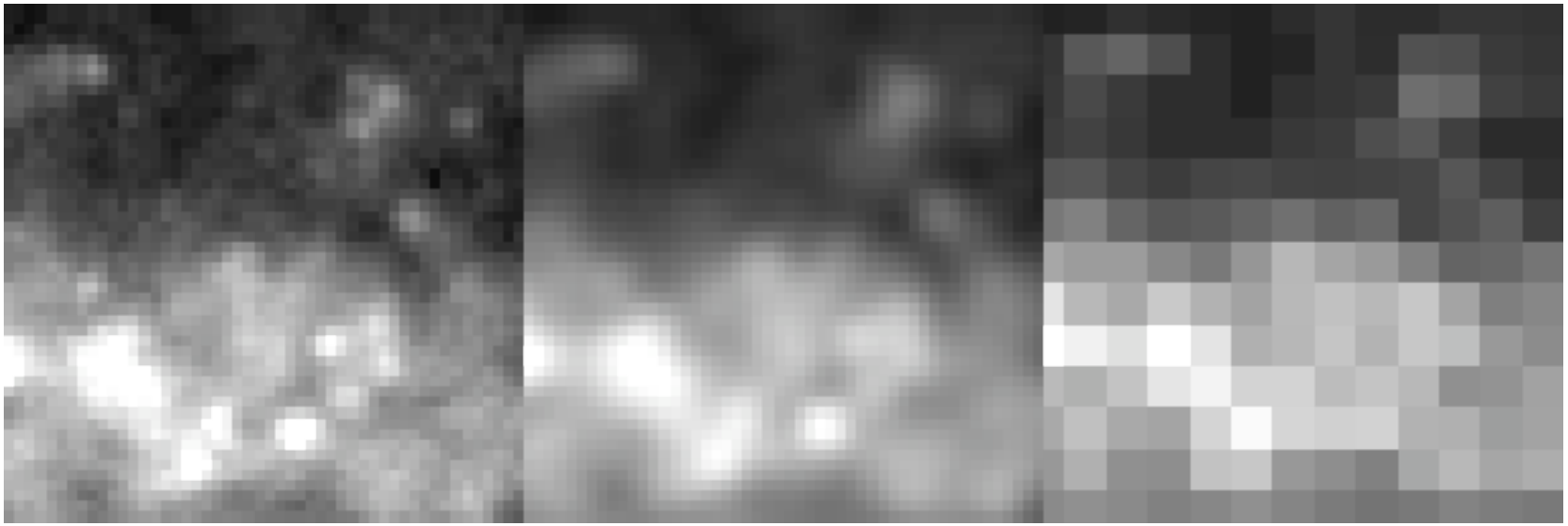

Fruchter & Hook 2000 (ADASS IX)

**SKY ⇒ TELESCOPE ⇒ DETECTOR**

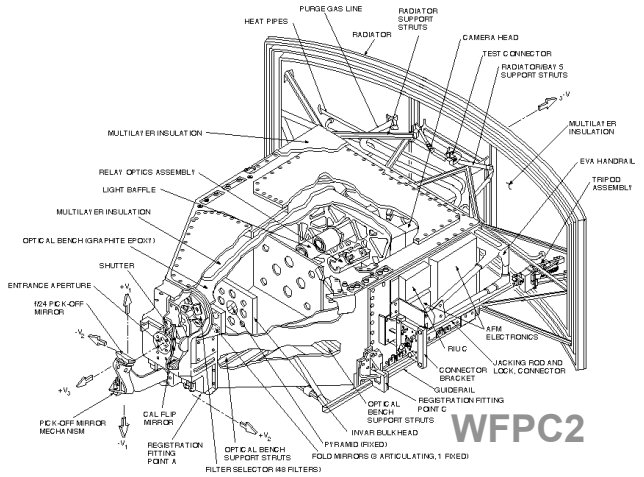

# Undersampled Point Spread Functions

HST WFPC2: WFC F555W 0.10 arcsecond pixels

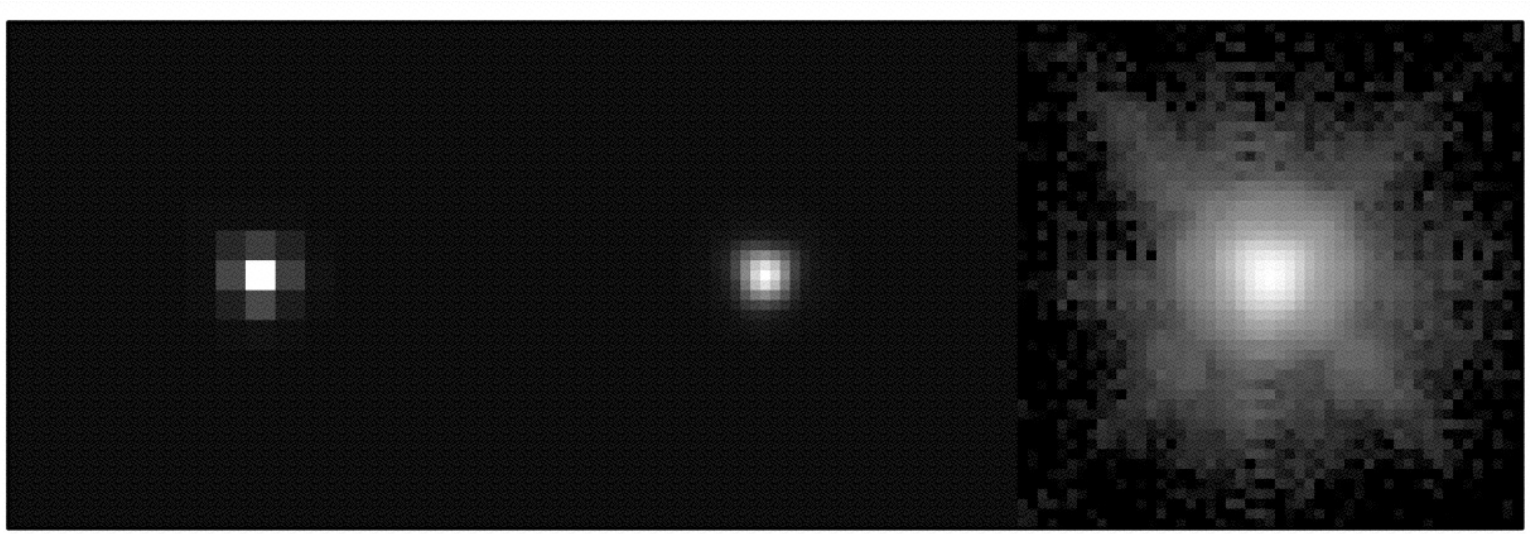


| original sampling | 3x3 supersampled | 3x3 supersampled |
|---|---|---|
| linear stretch | linear stretch | logarithmic stretch |

# Lossy Detectors

## Photometric Error: NIC3 F160W

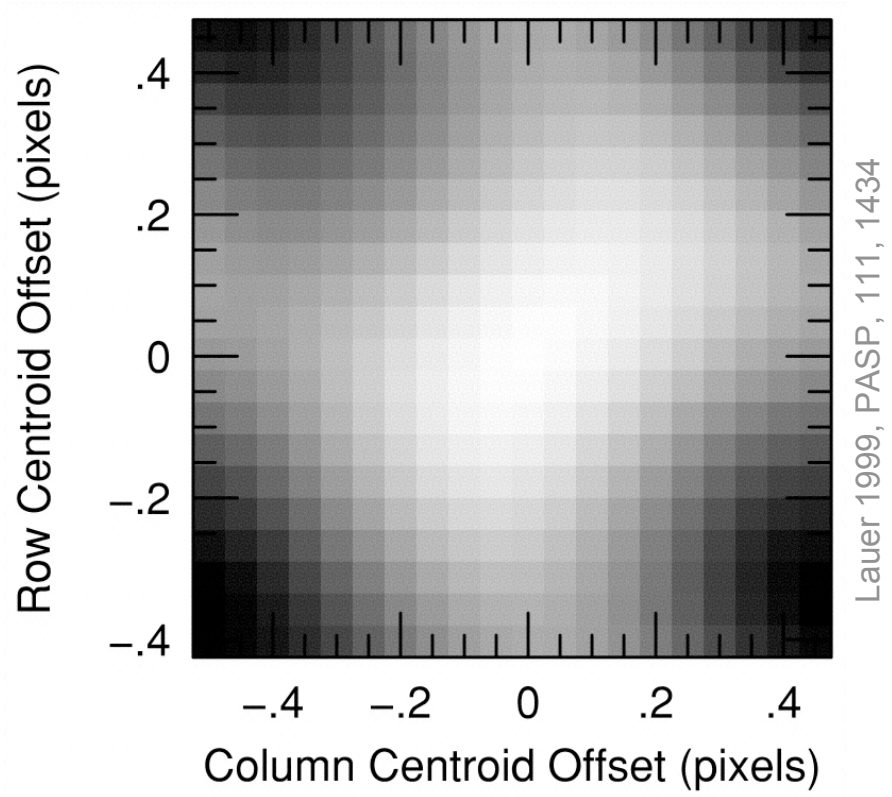


Lauer 1999, PASP, 111, 1434

white=0.12 mag excess, black=0.09 mag deficit

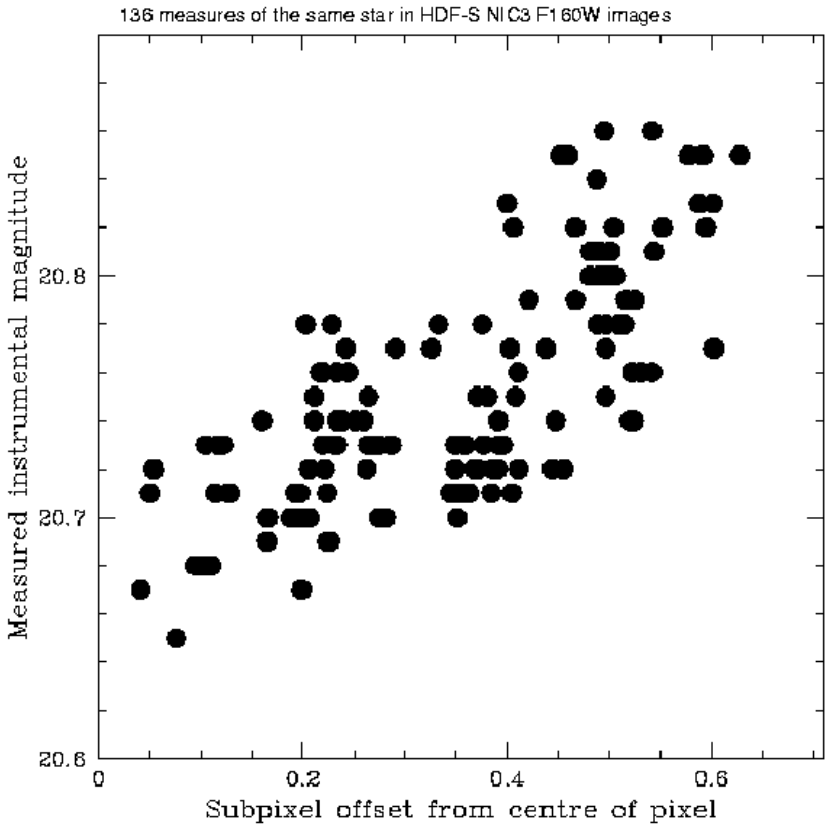


Fruchter & Hook 2000 (ADASS IX)

NICMOS

# Point Response Functions

Point Response Function ▼ ▼ Point Spread Function

$$\Psi \equiv \phi * \Lambda$$

▲ **D**etector **R**esponse **F**unction

$$\Psi_i(x_i, y_i) \equiv \int_{x_i-0.5}^{x_i+0.5} \int_{y_i-0.5}^{y_i+0.5} \phi(x, y)\, dx\, dy \quad \text{(for an ideal DRF)}$$

$$\mathrm{V} \equiv \int_{-\infty}^{\infty} \int_{-\infty}^{\infty} \Psi\, dx\, dy \lesssim 1$$

Volume ▲

$$\text{sharpness} \equiv \int_{-\infty}^{\infty} \int_{-\infty}^{\infty} \left( \frac{\Psi}{\mathrm{V}} \right)^2 dx\, dy$$

▲ normalized PRF

$$\beta \equiv \left[ \iint_{-\infty}^{\infty} \Psi^2\, dx\, dy \right]^{-1} = \frac{1}{\mathrm{V}^2\, \text{sharpness}}$$

Effective Background Area ▲

$$\mathcal{L} \equiv \sqrt{\frac{\beta\, \mathrm{V}^2}{4\pi}} = \frac{1}{\sqrt{4\pi\, \text{sharpness}}}$$

Critical-Sampling Scale Length ▲

# Performance Model based on Information Theory

# I. Photometry

$$
\begin{aligned}
\sigma^2_{\mathcal{E}:\,\mathrm{bright}} &\approx \left[\sum_{i=1}^{N} \frac{1}{\sigma_i^2}\left(\frac{\partial\, m_i}{\partial \mathcal{E}}\right)^2\right]^{-1} \\
&\approx \left[\sum_{i=1}^{N} \frac{1}{\mathcal{E}\mathrm{V}\tilde{\Psi}_i}\left(\frac{\partial}{\partial \mathcal{E}}\left[\,\mathcal{E}\mathrm{V}\tilde{\Psi}_i + \mathcal{B}\,\right]\right)^2\right]^{-1} \\
&= \left[\frac{1}{\mathcal{E}\mathrm{V}}\sum_{i=1}^{N} \frac{1}{\tilde{\Psi}_i}\left(\mathrm{V}\tilde{\Psi}_i\right)^2\right]^{-1} \\
&= \left[\frac{\mathrm{V}}{\mathcal{E}}\sum_{i=1}^{N} \tilde{\Psi}_i\right]^{-1} \\
&\approx \frac{\mathcal{E}}{\mathrm{V}}\left[\int_{-\infty}^{+\infty}\int_{-\infty}^{+\infty} \tilde{\Psi}\, dx\, dy\right]^{-1} \\
&\equiv \frac{\mathcal{E}}{\mathrm{V}}
\end{aligned}
$$

$$\sigma_{\rm rms} \equiv \sqrt{\frac{1}{N}\sum_{i=1}^{N}\sigma_i^2} \approx \sqrt{\mathcal{B}+\sigma_{\rm RON}^2}$$

$$\sigma^2_{\mathcal{E}:\,\rm faint} \approx \left[\sum_{i=1}^{N}\frac{1}{\sigma_i^2}\left(\frac{\partial m_i}{\partial \mathcal{E}}\right)^2\right]^{-1}$$

$$\approx \left[\sum_{i=1}^{N}\frac{1}{\sigma^2_{\rm rms}}\left(\frac{\partial}{\partial \mathcal{E}}\left[\mathcal{E}{\rm V}\tilde{\Psi}_i+\mathcal{B}\right]\right)^2\right]^{-1}$$

$$\equiv \sigma^2_{\rm rms}\left[\sum_{i=1}^{N}(\Psi_i)^2\right]^{-1}$$

$$\approx \sigma^2_{\rm rms}\left[\int_{-\infty}^{+\infty}\int_{-\infty}^{+\infty}\Psi^2\,dx\,dy\right]^{-1}$$

$$\equiv \beta\,\sigma^2_{\rm rms}$$

$$\approx \beta\,\left[\mathcal{B}+\sigma^2_{\rm RON}\right]$$

# Systematic Error: Poor Sky Measurement

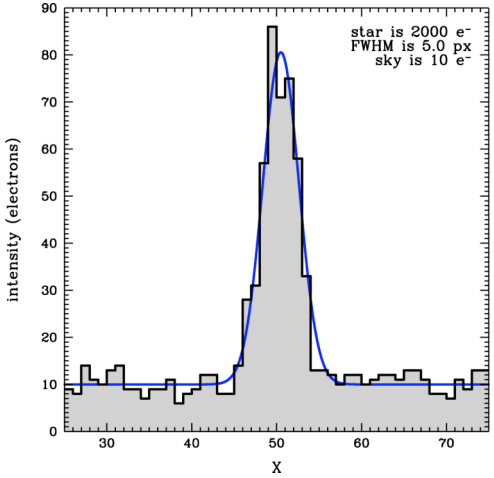


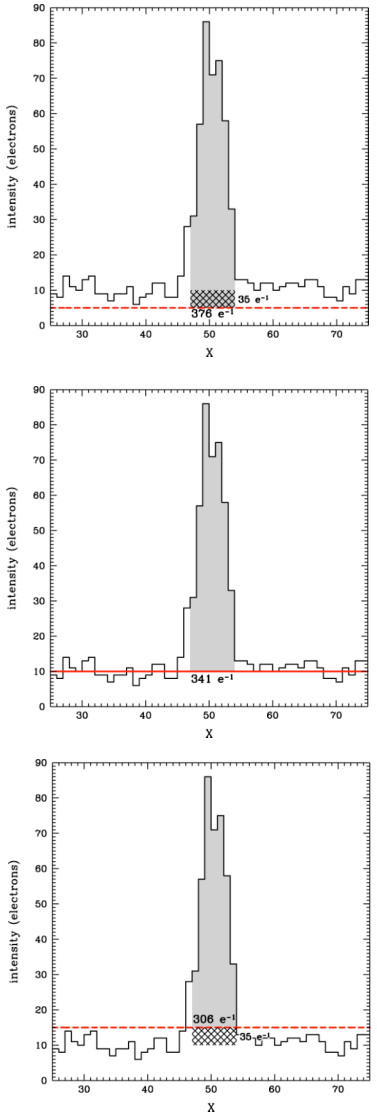


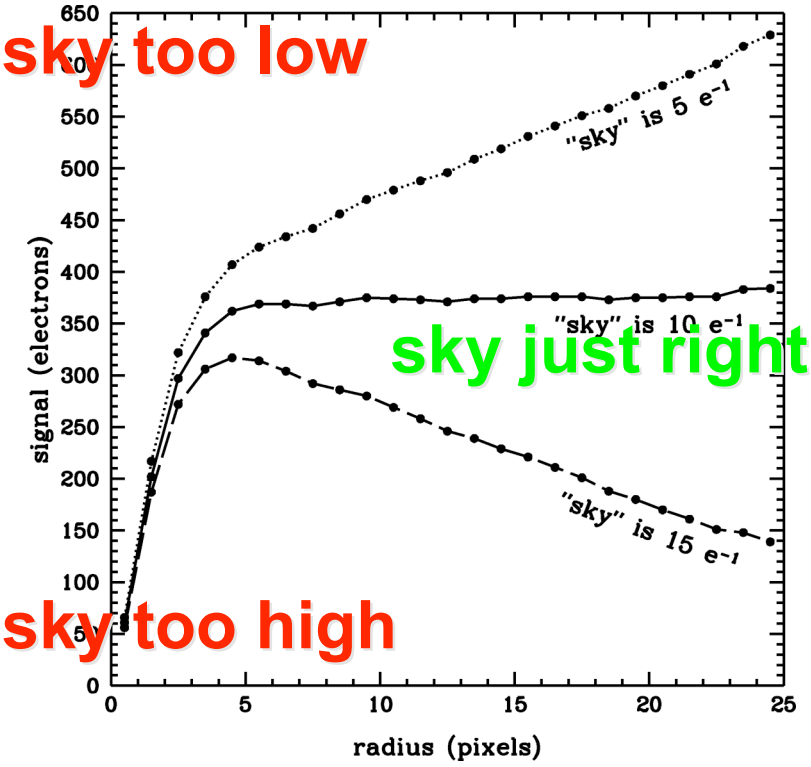

$$\sigma_{\mathcal{E}:\,\mathrm{faint}} \approx \sigma_{\mathrm{rms}}\sqrt{\beta} + \underline{\boldsymbol{\sigma_{\mathcal{B}}}\,\boldsymbol{\beta}}$$

$$\boldsymbol{\sigma_{\mathcal{B}}} \approx \left[\sum_{i=1}^{N} \frac{1}{\sigma_i^2}\left(\frac{\partial m_i}{\partial \mathcal{B}}\right)^2\right]^{-1/2}$$

$$\approx \left[\sum_{i=1}^{N} \frac{1}{\sigma_{\mathrm{rms}}^2}\left(\frac{\partial}{\partial \mathcal{B}}\left[\mathcal{E}\mathrm{V}\Psi_i + \mathcal{B}\right]\right)^2\right]^{-1/2}$$

$$= \sigma_{\mathrm{rms}}\left[\sum_{i=1}^{N} (1)^2\right]^{-1/2}$$

$$= \frac{\sigma_{\mathrm{rms}}}{\sqrt{N}}$$

$$\approx \sqrt{\frac{\mathcal{B} + \boldsymbol{\sigma_{\mathrm{RON}}^2}}{N}}$$

$$
\begin{aligned}
\boldsymbol{\sigma_{\mathcal{E}}}\text{: faint} &\approx \sigma_{\rm rms}\sqrt{\beta} + \sigma_{\mathcal{B}}\,\beta \\
&= \sqrt{\boldsymbol{\beta}}\left(1+\sqrt{\boldsymbol{\beta}/N}\right)\boldsymbol{\sigma_{\rm rms}} \\
&\approx \sqrt{\boldsymbol{\beta}}\left(1+\sqrt{\boldsymbol{\beta}/N}\right)\sqrt{\boldsymbol{\mathcal{B}}+\boldsymbol{\sigma^2_{\rm RON}}}
\end{aligned}
$$

$$
\begin{aligned}
\mathrm{S/N} &\lesssim \frac{\mathcal{E}}{\sigma_{\mathcal{E}}} \\
&\approx \frac{\mathcal{E}}{\sqrt{\sigma^2_{\mathcal{E}:\,\mathrm{bright}} + \sigma^2_{\mathcal{E}:\,\mathrm{faint}}}} \\
&\approx \frac{\mathcal{E}}{\sqrt{\frac{\mathcal{E}}{\mathrm{V}} + \beta\left(1+\sqrt{\beta/N}\right)^2 \sigma^2_{\mathrm{rms}}}} \\
&\approx \frac{\mathcal{E}}{\sqrt{\frac{\mathcal{E}}{\mathrm{V}} + \beta\left(1+\sqrt{\beta/N}\right)^2 \left[\,\mathcal{B} + \sigma^2_{\mathrm{RON}}\,\right]}}
\end{aligned}
$$

$$
\Delta\mathrm{mag} = \frac{5\,/\,\ln(100)}{\mathrm{SNR}} = \frac{2.5\log(e)}{\mathrm{SNR}} \approx \frac{1.0857}{\mathbf{S/N}}
$$

# II. Astrometry

$$\tilde{\mathsf{g}}(x,y;\mathcal{X},\mathcal{Y},\mathcal{S}) \equiv \frac{1}{2\pi\mathcal{S}^2} e^{-\left[\frac{(x-\mathcal{X})^2+(y-\mathcal{Y})^2}{2\mathcal{S}^2}\right]}$$

$$\tilde{\mathsf{g}}_i \equiv \tilde{\mathsf{g}}(x_i,y_i;\mathcal{X},\mathcal{Y},\mathcal{S})$$

$$\tilde{\mathsf{G}}_i \equiv \int_{x_i-0.5}^{x_i+0.5}\int_{y_i-0.5}^{y_i+0.5} \tilde{\mathsf{g}}(x,y;\mathcal{X},\mathcal{Y},\mathcal{S})\,dx\,dy$$

$$\tilde{\mathsf{G}}_i \approx \tilde{\mathsf{g}}_i \quad (\text{for } \mathcal{S} \gg 1\ )$$

$$m_i \equiv \mathcal{E}\mathrm{V}\tilde{\mathsf{G}}_i + \mathcal{B}$$

$$
\begin{aligned}
\sigma^2_{\mathcal{X}}\text{: bright} \quad &\approx \left[\sum_{i=1}^{N} \frac{1}{\sigma_i^2}\left(\frac{\partial m_i}{\partial \mathcal{X}}\right)^2\right]^{-1} \\
&\approx \left[\sum_{i=1}^{N} \frac{1}{\mathcal{E}\mathrm{V}\tilde{\mathrm{G}}_i}\left(\frac{\partial}{\partial \mathcal{X}}\left[\mathcal{E}\mathrm{V}\tilde{\mathrm{G}}_i + \mathcal{B}\right]\right)^2\right]^{-1} \\
&\approx \left[\sum_{i=1}^{N} \frac{1}{\mathcal{E}\mathrm{V}\tilde{\mathrm{g}}_i}\left(\mathcal{E}V\frac{\partial}{\partial \mathcal{X}}\tilde{\mathrm{g}}_i\right)^2\right]^{-1} \\
&= \left[\sum_{i=1}^{N} \frac{1}{\mathcal{E}\mathrm{V}\tilde{\mathrm{g}}_i}\left(\mathcal{E}V\tilde{\mathrm{g}}_i\frac{x_i - \mathcal{X}}{\mathcal{S}^2}\right)^2\right]^{-1} \\
&\approx \frac{\mathcal{S}^4}{\mathcal{E}\mathrm{V}}\left[\iint_{-\infty}^{+\infty} \tilde{\mathrm{g}}(x,y;\mathcal{X},\mathcal{Y},\mathcal{S})\,(x-\mathcal{X})^2\,dx\,dy\right]^{-1} \\
&= \frac{\mathcal{S}^2}{\mathcal{E}\mathrm{V}} \\
&\approx \frac{\mathcal{L}^2}{\mathcal{E}\mathrm{V}}, \quad \text{where } \mathcal{L} \equiv \sqrt{\frac{\beta\mathrm{V}^2}{4\pi}} \equiv \sqrt{\frac{\tilde{\beta}}{4\pi}} \equiv \frac{1}{\sqrt{4\pi\,\textbf{sharpness}}}
\end{aligned}
$$

= 1 if critically sampled

$$
\begin{aligned}
\boldsymbol{\sigma^2_{\mathcal{X}}}\text{: faint} &\approx \left[\sum_{i=1}^{N} \frac{1}{\sigma_i^2}\left(\frac{\partial m_i}{\partial \mathcal{X}}\right)^2\right]^{-1} \\
&\approx \left[\sum_{i=1}^{N} \frac{1}{\sigma^2_{\rm rms}}\left(\frac{\partial}{\partial \mathcal{X}}\left[\mathcal{E}\mathrm{V}\tilde{\mathrm{G}}_i + \mathcal{B}\right]\right)^2\right]^{-1} \\
&\approx \sigma^2_{\rm rms}\left[\sum_{i=1}^{N}\left(\mathcal{E}V\frac{\partial}{\partial \mathcal{X}}\tilde{\mathrm{g}}_i\right)^2\right]^{-1} \\
&= \sigma^2_{\rm rms}\left[\sum_{i=1}^{N}\left(\mathcal{E}V\tilde{\mathrm{g}}_i\frac{x_i-\mathcal{X}}{\mathcal{S}^2}\right)^2\right]^{-1} \\
&\approx \sigma^2_{\rm rms}\frac{S^4}{\mathcal{E}^2\mathrm{V}^2}\left[\iint_{-\infty}^{+\infty}\left[\tilde{\mathrm{g}}(x,y;\mathcal{X},\mathcal{Y},\mathcal{S})(x-\mathcal{X})\right]^2 dx\,dy\right]^{-1} \\
&= 8\,\pi\,\sigma^2_{\rm rms}\frac{S^4}{\mathcal{E}^2\mathrm{V}^2} \\
&\approx 8\,\pi\,\boldsymbol{\sigma^2_{\rm rms}}\left(\frac{\boldsymbol{\mathcal{L}}^2}{\boldsymbol{\mathcal{E}}\,\mathrm{V}}\right)^2 \approx 8\,\pi\,\boldsymbol{\sigma^2_{\rm rms}}\left(\boldsymbol{\sigma^2_{\mathcal{X}}}\text{: bright}\right)^2
\end{aligned}
$$

$$
\begin{aligned}
\sigma_{\mathcal{X}} &\approx \sqrt{\sigma^2_{\mathcal{X}:\,\mathrm{bright}} + \sigma^2_{\mathcal{X}:\,\mathrm{faint}}} \\
&\approx \sqrt{\frac{\mathcal{L}^2}{\mathcal{E}\,\mathrm{V}}\left[1 + 8\,\pi\,\sigma^2_{\mathrm{rms}}\,\frac{\mathcal{L}^2}{\mathcal{E}\,\mathrm{V}}\right]} \\
&\approx \sqrt{\frac{\mathcal{L}^2}{\mathcal{E}\,\mathrm{V}}\left[1 + 8\,\pi\,\left(\mathcal{B} + \sigma^2_{\mathrm{RON}}\right)\frac{\mathcal{L}^2}{\mathcal{E}\,\mathrm{V}}\right]} \\
\sigma_{\mathcal{Y}} &= \sigma_{\mathcal{X}}
\end{aligned}
$$

# III. Relationship Between Astrometric and Photometric Errors

**Bright stars:**

$$\frac{\sigma_{\mathcal{X}}}{\mathcal{L}} = \frac{\sigma_{\mathcal{E}}}{\mathcal{E}}$$

**Faint stars:**

$$\frac{\sigma_{\mathcal{X}}}{\mathcal{L}} \approx \left(\frac{\sigma_{\mathcal{E}}}{\mathcal{E}}\right) \frac{\sqrt{2}}{1+\sqrt{\beta/N}}$$

# IV. Performance Model

background level ▼ ▼ volume of Point Response Function

$$m_i \equiv \mathcal{B} + \mathcal{E}\mathrm{V}\tilde{\Psi}_i$$

pixel value ▲ ▲ normalized PRF

stellar intensity [electrons] ▲

$$\tilde{\Psi}_i(x_i, y_i) \equiv \int_{x_i-0.5}^{x_i+0.5} \int_{y_i-0.5}^{y_i+0.5} \phi(x, y)\, dx\, dy \quad (\text{ideal DRF: } \mathrm{V} \equiv 1)$$

▲ Point Spread Function

$$\mathrm{S/N} \equiv \frac{\mathcal{E}}{\sigma_{\mathcal{E}}} \approx \frac{\mathcal{E}}{\sqrt{\frac{\mathcal{E}}{\mathrm{V}} + \beta\left(1 + \sqrt{\beta/N}\right)^2 \left[\mathcal{B} + \sigma_{\mathrm{RON}}^2\right]}}$$

signal-to-noise ratio ▲ ▲ readout noise

▲ aperture size [pixels]

▲ Effective Background Area

$$\Delta\mathrm{mag} \approx \frac{1.0857}{\mathrm{S/N}}$$

▼ Critical-Sampling Scale Length

$$\sigma_{\mathcal{X}} \approx \sqrt{\frac{\mathcal{L}^2}{\mathcal{E}\mathrm{V}}\left[1 + 8\pi\left(\mathcal{B} + \sigma_{\mathrm{RON}}^2\right)\frac{\mathcal{L}^2}{\mathcal{E}\mathrm{V}}\right]}$$

$$\sigma_{\mathcal{Y}} = \sigma_{\mathcal{X}}$$

Mon. Not. R. Astron. Soc. **361,** 861–878 (2005) doi:10.1111/j.1365-2966.2005.09208.x

**Stellar photometry and astrometry with discrete point spread functions**

Kenneth J. Mighell★
*National Optical Astronomy Observatory, 950 North Cherry Avenue, Tucson, AZ 85719, USA*

# Photometry and Astrometry with Discrete PSFs

# What is a discrete PSF?

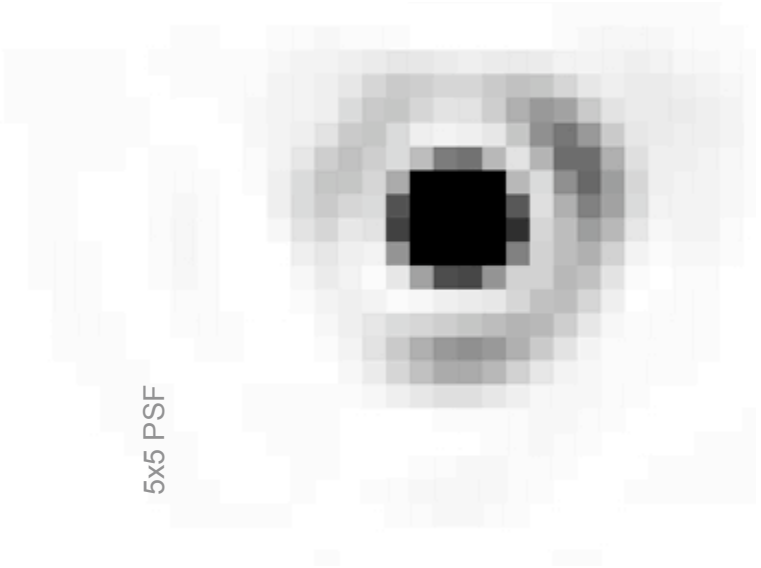


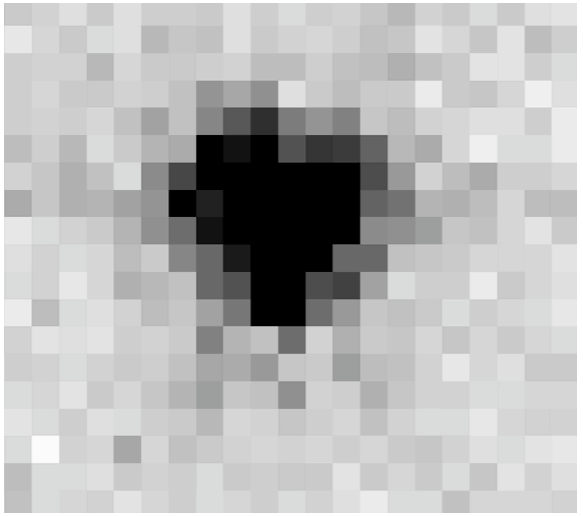



# Nonlinear Least Squares Theory

$$\chi^2(\mathbf{p}) \equiv \sum_{i=1}^{N} \frac{1}{\sigma_i^2}\left(z_i - m_i\right)^2$$

▲parameter vector ▲data ▲model ▲measurement error

$$\chi^2(\mathbf{p}+\boldsymbol{\delta}) = \sum_{n=0}^{\infty} \frac{1}{n!}(\boldsymbol{\delta}\cdot\nabla)^n \chi^2(\mathbf{p})$$

▲correction vector

$$\approx \chi^2(\mathbf{p}) + \boldsymbol{\delta}\cdot\nabla\chi^2(\mathbf{p}) + \frac{1}{2}\boldsymbol{\delta}\cdot\boldsymbol{H}\cdot\boldsymbol{\delta}$$

▲Hessian matrix

$$[\mathbf{H}]_{\mathbf{jk}} \equiv \frac{\partial^2}{\partial \mathbf{a_j}\partial \mathbf{a_k}}\chi^2(\mathbf{p})$$

$$\boldsymbol{H}\cdot\boldsymbol{\delta} = -\nabla\chi^2(\mathbf{p})$$

$$\mathbf{p}' = \mathbf{p} + \boldsymbol{\delta}$$

$$\sigma_{\mathbf{j}} \approx \sqrt{[\mathbf{H}^{-1}]_{jj}} = \left[\sum_{i=1}^{N} \frac{1}{\sigma_i^2}\left(\frac{\partial m_i}{\partial p_j}\right)^2\right]^{-1/2}$$

▲measurement error

# How does one move a PSF?

Analytical PSFs: Just compute the PSF at the desired location in the observational model.

Numerical PSFs: Take the reference numerical PSF and shift it to the desired location using a perfect 2-d interpolation function. OK… but how is that done in practice?

Solution

*Use the following 21-pixel-wide damped sinc function:*

$$f^{\rm shifted}(\delta x) \equiv \sum_{i=-10}^{10} f(x_i) \frac{\sin\Big(\pi(x_i - \delta x)\Big)}{\pi(x_i - \delta x)} \exp\left(-\frac{(x_i - \delta x)^2}{(3.25)^2}\right)$$

**Note: The 2-d sinc function is separable in $x$ and $y$.**

# Hessian matrix

Standard definition for model $m = \mathcal{E} \, \mathrm{V} \, \tilde{\Psi}(\mathcal{X}, \mathcal{Y}) + \mathcal{B}$ and $N$ data values:

$$\boldsymbol{H} \equiv \begin{bmatrix} \sum_{i=1}^{N} \frac{1}{\sigma_i^2} \frac{\partial^2 m_i}{\partial \mathcal{E} \partial \mathcal{E}} & \sum_{i=1}^{N} \frac{1}{\sigma_i^2} \frac{\partial^2 m_i}{\partial \mathcal{E} \partial \mathcal{X}} & \sum_{i=1}^{N} \frac{1}{\sigma_i^2} \frac{\partial^2 m_i}{\partial \mathcal{E} \partial \mathcal{Y}} & \sum_{i=1}^{N} \frac{1}{\sigma_i^2} \frac{\partial^2 m_i}{\partial \mathcal{E} \partial \mathcal{B}} \\ \sum_{i=1}^{N} \frac{1}{\sigma_i^2} \frac{\partial^2 m_i}{\partial \mathcal{X} \partial \mathcal{E}} & \sum_{i=1}^{N} \frac{1}{\sigma_i^2} \frac{\partial^2 m_i}{\partial \mathcal{X} \partial \mathcal{X}} & \sum_{i=1}^{N} \frac{1}{\sigma_i^2} \frac{\partial^2 m_i}{\partial \mathcal{X} \partial \mathcal{Y}} & \sum_{i=1}^{N} \frac{1}{\sigma_i^2} \frac{\partial^2 m_i}{\partial \mathcal{X} \partial \mathcal{B}} \\ \sum_{i=1}^{N} \frac{1}{\sigma_i^2} \frac{\partial^2 m_i}{\partial \mathcal{Y} \partial \mathcal{E}} & \sum_{i=1}^{N} \frac{1}{\sigma_i^2} \frac{\partial^2 m_i}{\partial \mathcal{Y} \partial \mathcal{X}} & \sum_{i=1}^{N} \frac{1}{\sigma_i^2} \frac{\partial^2 m_i}{\partial \mathcal{Y} \partial \mathcal{Y}} & \sum_{i=1}^{N} \frac{1}{\sigma_i^2} \frac{\partial^2 m_i}{\partial \mathcal{Y} \partial \mathcal{B}} \\ \sum_{i=1}^{N} \frac{1}{\sigma_i^2} \frac{\partial^2 m_i}{\partial \mathcal{B} \partial \mathcal{E}} & \sum_{i=1}^{N} \frac{1}{\sigma_i^2} \frac{\partial^2 m_i}{\partial \mathcal{B} \partial \mathcal{X}} & \sum_{i=1}^{N} \frac{1}{\sigma_i^2} \frac{\partial^2 m_i}{\partial \mathcal{B} \partial \mathcal{Y}} & \sum_{i=1}^{N} \frac{1}{\sigma_i^2} \frac{\partial^2 m_i}{\partial \mathcal{B} \partial \mathcal{B}} \end{bmatrix}$$

# Hessian matrix

Robust approximation for model $\boldsymbol{m = \mathcal{E}\,\mathrm{V}\,\tilde{\Psi}(\mathcal{X},\mathcal{Y}) + \mathcal{B}}$ and $N$ data values:

$$\boldsymbol{H} \approx \begin{bmatrix} \sum_{i=1}^{N} \frac{1}{\sigma_i^2} \frac{\partial m_i}{\partial \mathcal{E}} \frac{\partial m_i}{\partial \mathcal{E}} & \sum_{i=1}^{N} \frac{1}{\sigma_i^2} \frac{\partial m_i}{\partial \mathcal{E}} \frac{\partial m_i}{\partial \mathcal{X}} & \sum_{i=1}^{N} \frac{1}{\sigma_i^2} \frac{\partial m_i}{\partial \mathcal{E}} \frac{\partial m_i}{\partial \mathcal{Y}} & \sum_{i=1}^{N} \frac{1}{\sigma_i^2} \frac{\partial m_i}{\partial \mathcal{E}} \frac{\partial m_i}{\partial \mathcal{B}} \\ \sum_{i=1}^{N} \frac{1}{\sigma_i^2} \frac{\partial m_i}{\partial \mathcal{X}} \frac{\partial m_i}{\partial \mathcal{E}} & \sum_{i=1}^{N} \frac{1}{\sigma_i^2} \frac{\partial m_i}{\partial \mathcal{X}} \frac{\partial m_i}{\partial \mathcal{X}} & \sum_{i=1}^{N} \frac{1}{\sigma_i^2} \frac{\partial m_i}{\partial \mathcal{X}} \frac{\partial m_i}{\partial \mathcal{Y}} & \sum_{i=1}^{N} \frac{1}{\sigma_i^2} \frac{\partial m_i}{\partial \mathcal{X}} \frac{\partial m_i}{\partial \mathcal{B}} \\ \sum_{i=1}^{N} \frac{1}{\sigma_i^2} \frac{\partial m_i}{\partial \mathcal{Y}} \frac{\partial m_i}{\partial \mathcal{E}} & \sum_{i=1}^{N} \frac{1}{\sigma_i^2} \frac{\partial m_i}{\partial \mathcal{Y}} \frac{\partial m_i}{\partial \mathcal{X}} & \sum_{i=1}^{N} \frac{1}{\sigma_i^2} \frac{\partial m_i}{\partial \mathcal{Y}} \frac{\partial m_i}{\partial \mathcal{Y}} & \sum_{i=1}^{N} \frac{1}{\sigma_i^2} \frac{\partial m_i}{\partial \mathcal{Y}} \frac{\partial m_i}{\partial \mathcal{B}} \\ \sum_{i=1}^{N} \frac{1}{\sigma_i^2} \frac{\partial m_i}{\partial \mathcal{B}} \frac{\partial m_i}{\partial \mathcal{E}} & \sum_{i=1}^{N} \frac{1}{\sigma_i^2} \frac{\partial m_i}{\partial \mathcal{B}} \frac{\partial m_i}{\partial \mathcal{X}} & \sum_{i=1}^{N} \frac{1}{\sigma_i^2} \frac{\partial m_i}{\partial \mathcal{B}} \frac{\partial m_i}{\partial \mathcal{Y}} & \sum_{i=1}^{N} \frac{1}{\sigma_i^2} \frac{\partial m_i}{\partial \mathcal{B}} \frac{\partial m_i}{\partial \mathcal{B}} \end{bmatrix}$$

# Jacobian matrix

For model $m_i \equiv \mathcal{E}\,\mathrm{V}\,\tilde{\Psi}_i(\mathcal{X},\mathcal{Y}) + \mathcal{B}$ with $N$ data values,

$$\boldsymbol{J} \equiv \begin{bmatrix} \frac{\partial m_1}{\partial \mathcal{E}} & \frac{\partial m_1}{\partial \mathcal{X}} & \frac{\partial m_1}{\partial \mathcal{Y}} & \frac{\partial m_1}{\partial \mathcal{B}} \\ \frac{\partial m_2}{\partial \mathcal{E}} & \frac{\partial m_2}{\partial \mathcal{X}} & \frac{\partial m_2}{\partial \mathcal{Y}} & \frac{\partial m_2}{\partial \mathcal{B}} \\ \frac{\partial m_3}{\partial \mathcal{E}} & \frac{\partial m_3}{\partial \mathcal{X}} & \frac{\partial m_3}{\partial \mathcal{Y}} & \frac{\partial m_3}{\partial \mathcal{B}} \\ \vdots & \vdots & \vdots & \vdots \\ \frac{\partial m_N}{\partial \mathcal{E}} & \frac{\partial m_N}{\partial \mathcal{X}} & \frac{\partial m_N}{\partial \mathcal{Y}} & \frac{\partial m_N}{\partial \mathcal{B}} \end{bmatrix}$$

▲ ▲ ▲ ▲

**Each column forms an image**

# Derivatives of the PRF

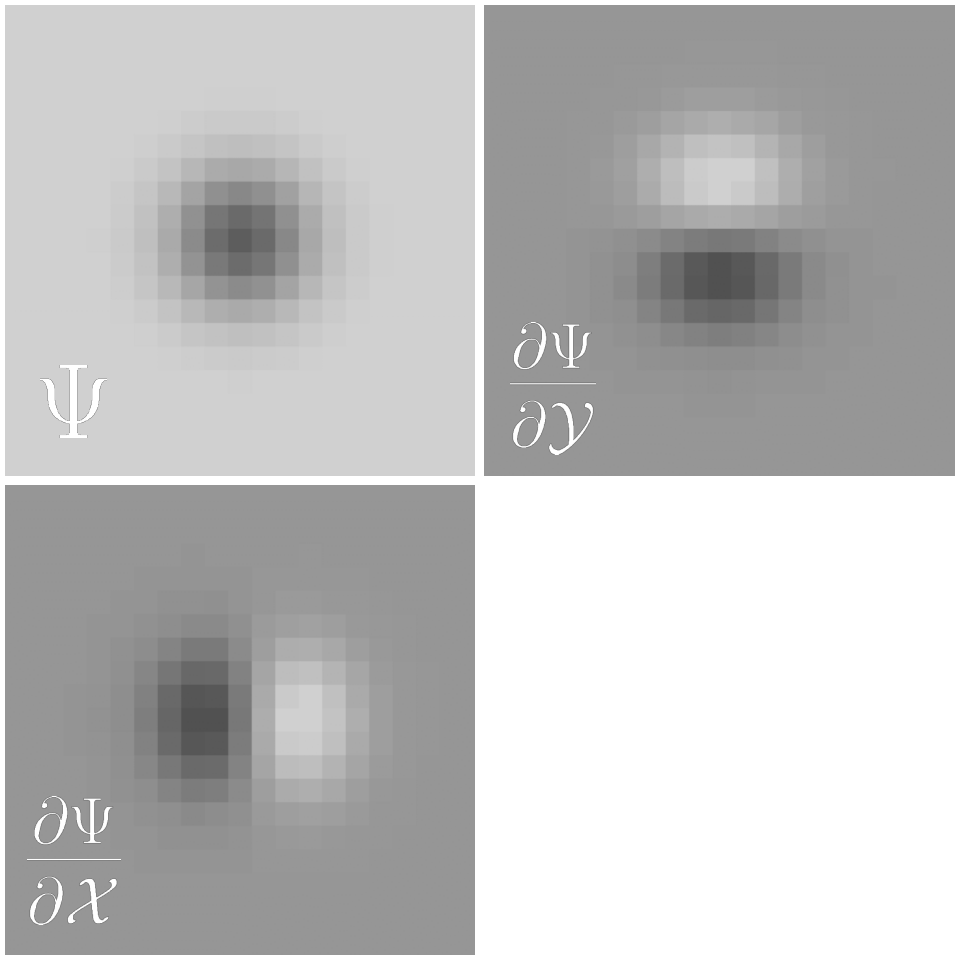

# Analytical Derivatives

$$\Psi_i(x_i, y_i; \mathcal{E}, \mathcal{X}, \mathcal{Y}, \mathcal{S}) \equiv \int_{x_i-0.5}^{x_i+0.5} \int_{y_i-0.5}^{y_i+0.5} \phi(x, y; \mathcal{E}, \mathcal{X}, \mathcal{Y}, \mathcal{S})\, dx\, dy \quad \text{(ideal DRF)}$$

$$\approx \frac{1}{\eta^2} \sum_{j=1}^{\eta} \sum_{k=1}^{\eta} \phi(x_i - \Delta + j\delta,\ y_i - \Delta + k\delta; \mathcal{E}, \mathcal{X}, \mathcal{Y}, \mathcal{S})$$

$$\text{where} \quad \Delta \equiv \frac{\eta + 1}{2\eta} \quad \text{and} \quad \delta \equiv \frac{1}{\eta}$$

$$\frac{\partial}{\partial \mathcal{X}} \Psi_i \equiv \frac{\partial}{\partial \mathcal{X}} \int_{x_i-0.5}^{x_i+0.5} \int_{y_i-0.5}^{y_i+0.5} \phi(x, y; \mathcal{E}, \mathcal{X}, \mathcal{Y}, \mathcal{S})\, dx\, dy \quad \text{(ideal DRF)}$$

$$\approx \frac{1}{\eta^2} \sum_{j=1}^{\eta} \sum_{k=1}^{\eta} \frac{\partial}{\partial \mathcal{X}} \phi(x_i - \Delta + j\delta,\ y_i - \Delta + k\delta; \mathcal{E}, \mathcal{X}, \mathcal{Y}, \mathcal{S})$$

$$\frac{\partial}{\partial \mathcal{Y}} \Psi_i \equiv \frac{\partial}{\partial \mathcal{Y}} \int_{x_i-0.5}^{x_i+0.5} \int_{y_i-0.5}^{y_i+0.5} \phi(x, y; \mathcal{E}, \mathcal{X}, \mathcal{Y}, \mathcal{S})\, dx\, dy \quad \text{(ideal DRF)}$$

$$\approx \frac{1}{\eta^2} \sum_{j=1}^{\eta} \sum_{k=1}^{\eta} \frac{\partial}{\partial \mathcal{Y}} \phi(x_i - \Delta + j\delta,\ y_i - \Delta + k\delta; \mathcal{E}, \mathcal{X}, \mathcal{Y}, \mathcal{S})$$

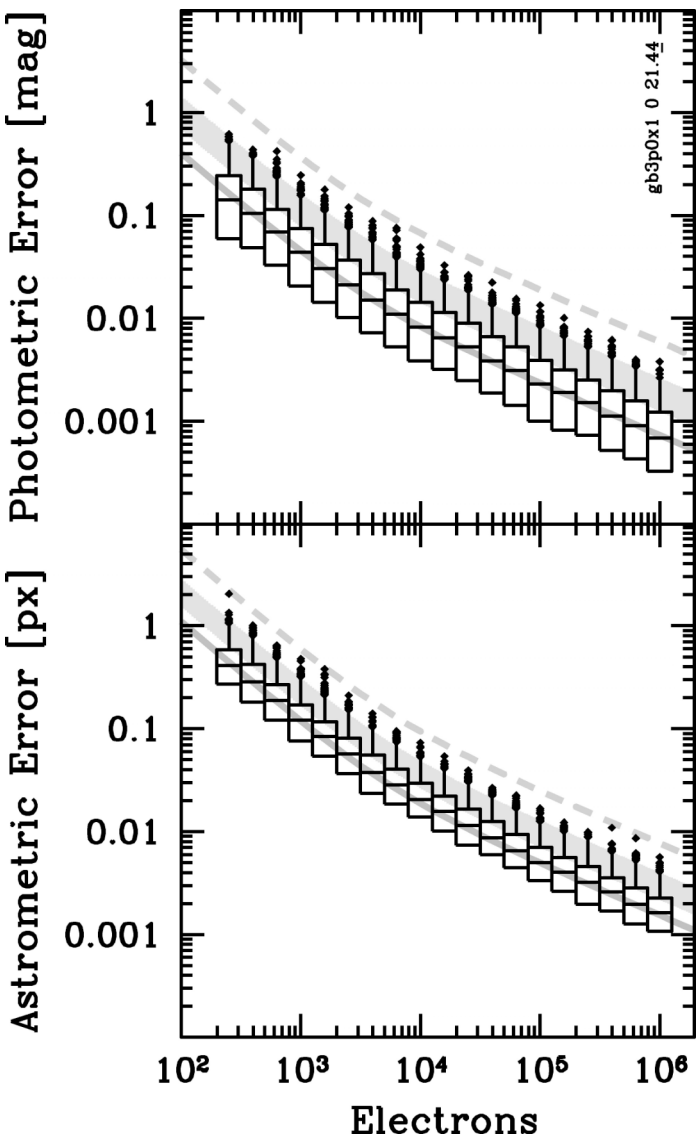


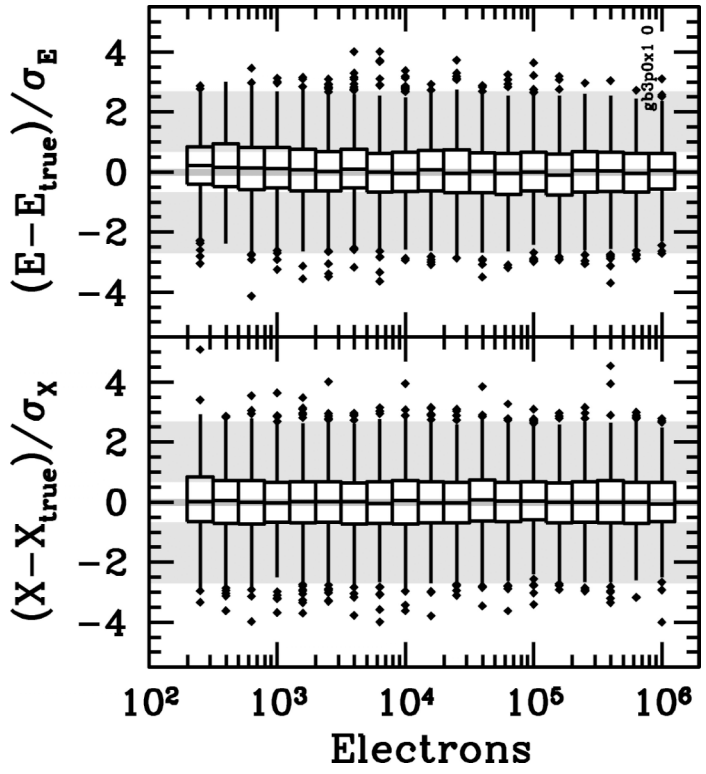


Data: Analytical Gaussian FWHM=3.0 px
Model: Analytical Gaussian FWHM=3.0 px

# Numerical Derivatives

The mathematics of determining the position partial derivatives of the observational model with respect to the $x$ and $y$ direction vectors is exactly the same with analytical or numerical PSFs. The implementation methodology, however, is significantly different. The position partial derivatives of numerical PSFs can be determined using numerical differentiation techniques on the numerical PSF. Numerical experiments have shown that the following five-point differentiation formula works well with numerical PSFs:

$$f'(x_i) \approx \frac{1}{12}\left[f(x_{i-2}) - 8f(x_{i-1}) + 8f(x_{i+1}) - f(x_{i+2})\right]$$

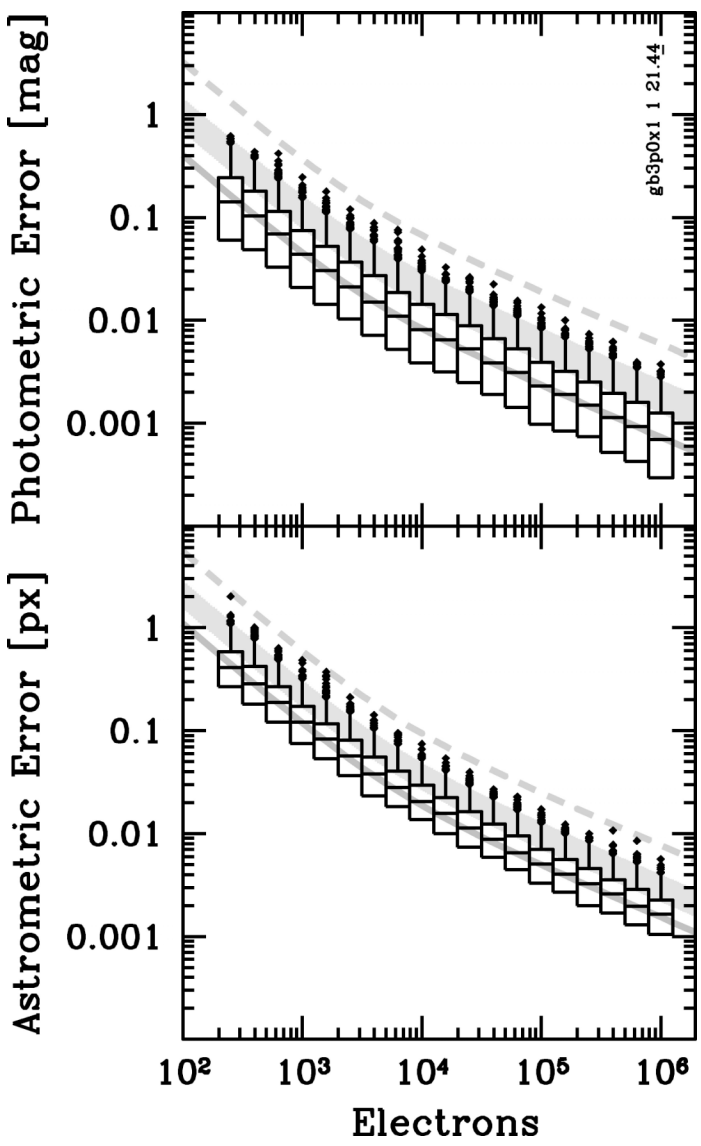


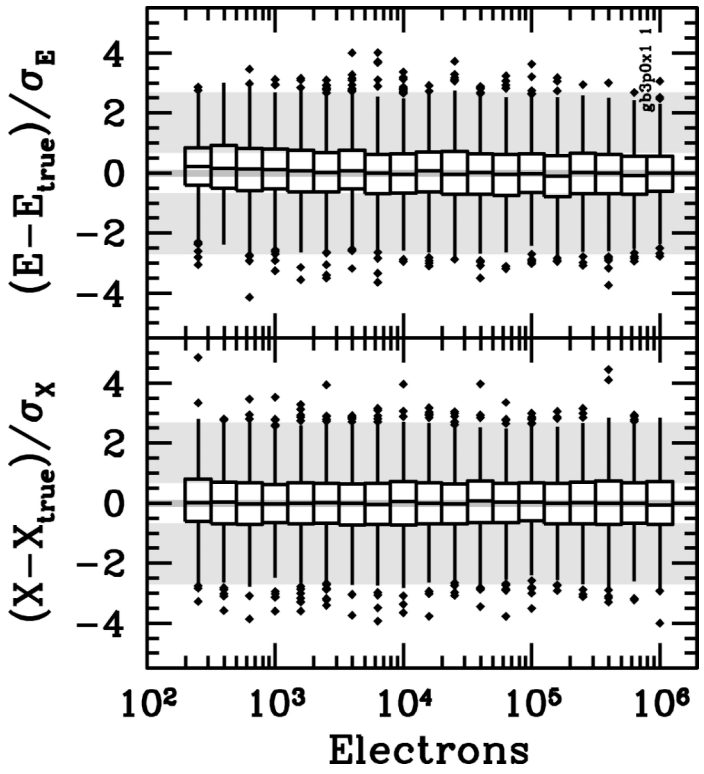


Data: Analytical Gaussian FWHM=3.0 px
Model: Numerical Gaussian FWHM=3.0 px

# Why does this work so well?

## Photon Noise

▲and That's A Good Thing®

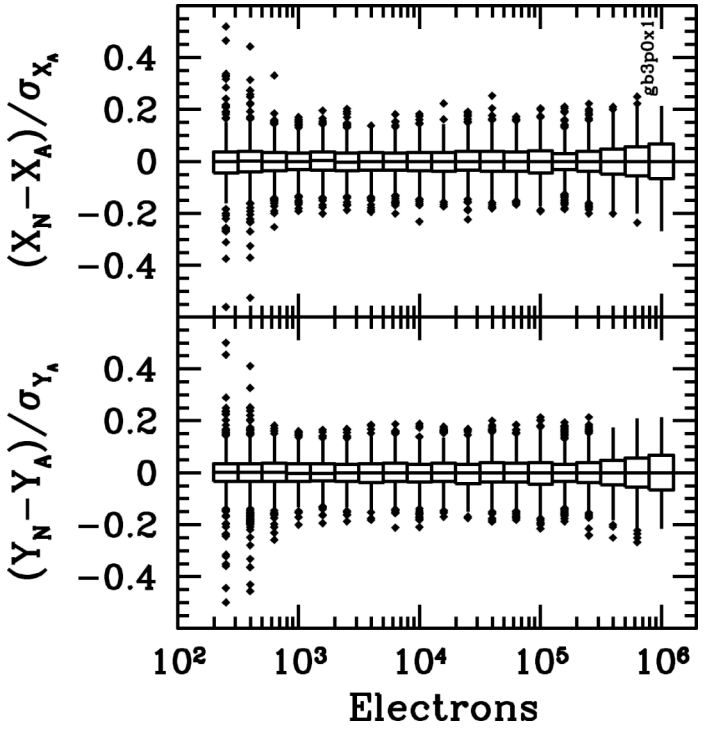


**Computational noise < 1/15th photon noise**

# Inefficient Detectors

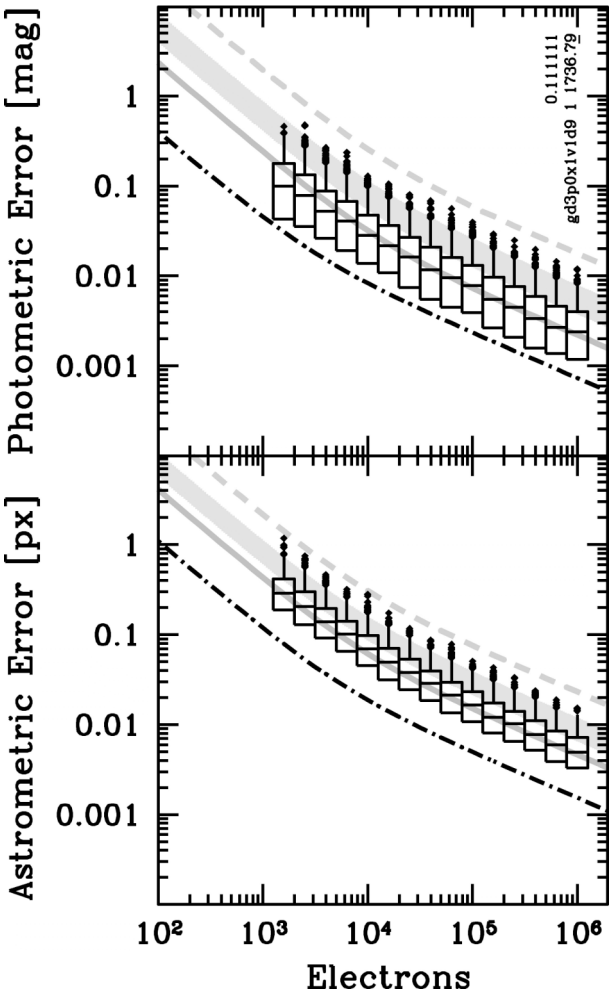


Data: Analytical Gaussian FWHM=3.0 px & V=1/9
Model: Numerical Gaussian FWHM=3.0 px

# Problem: Undersampled PRFs

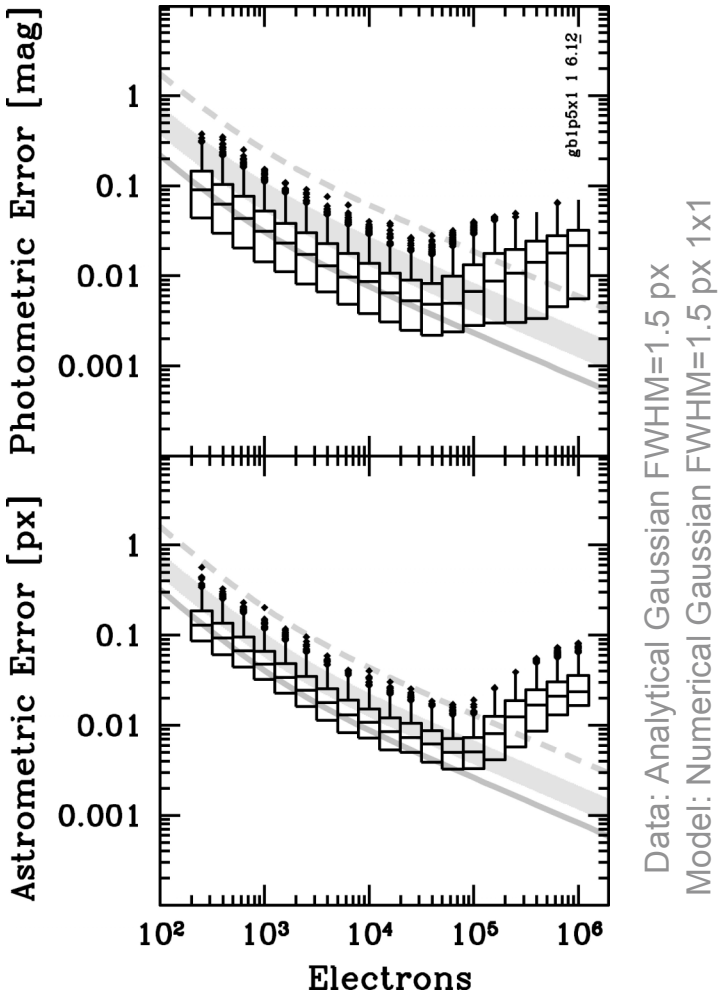

# Source of the problem: *Negative flux values* caused by shifting an undersampled PSF !

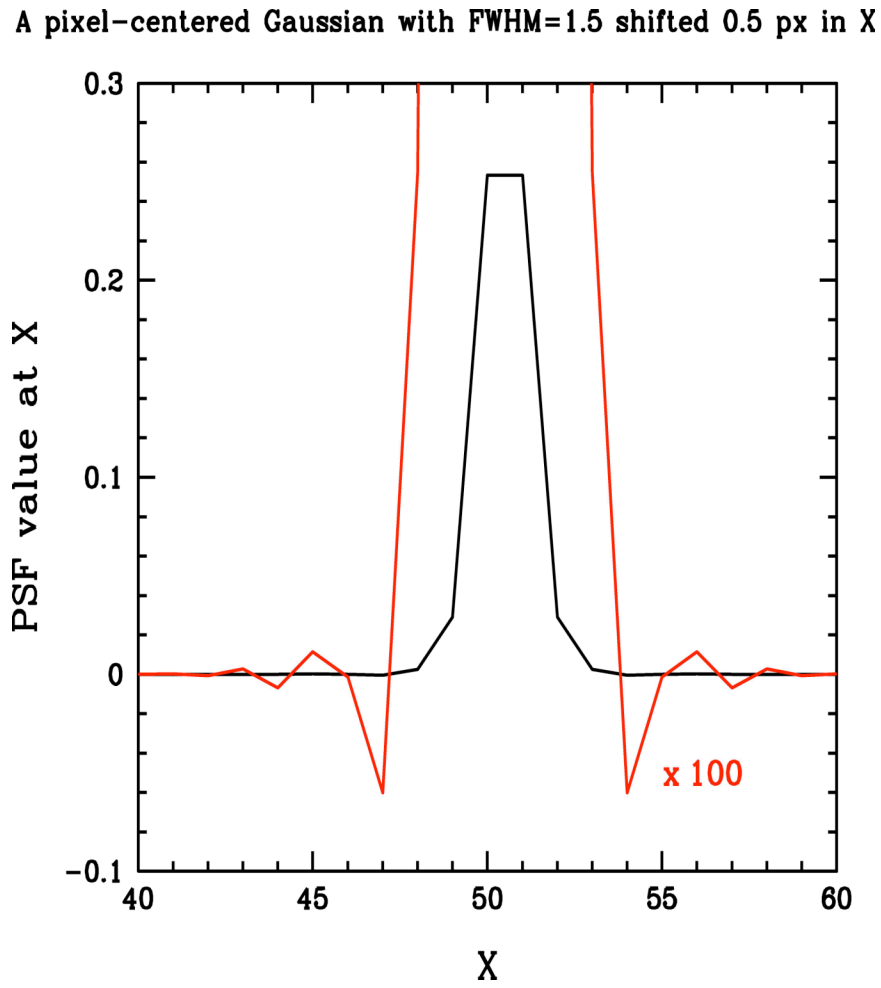

## Question: But why did it work for faint stars?

**Because one need lots of photons to properly sample the higher spatial frequencies of a PSF!**

# Solution: Use Supersampled PSFs !

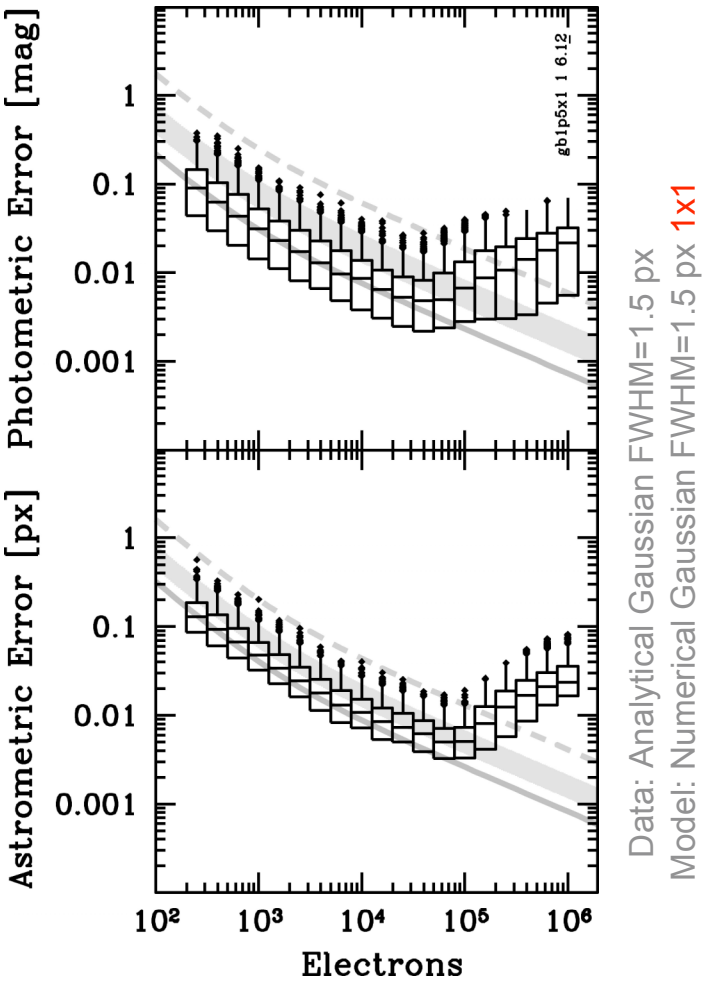


Data: Analytical Gaussian FWHM=1.5 px
Model: Numerical Gaussian FWHM=1.5 px 1x1

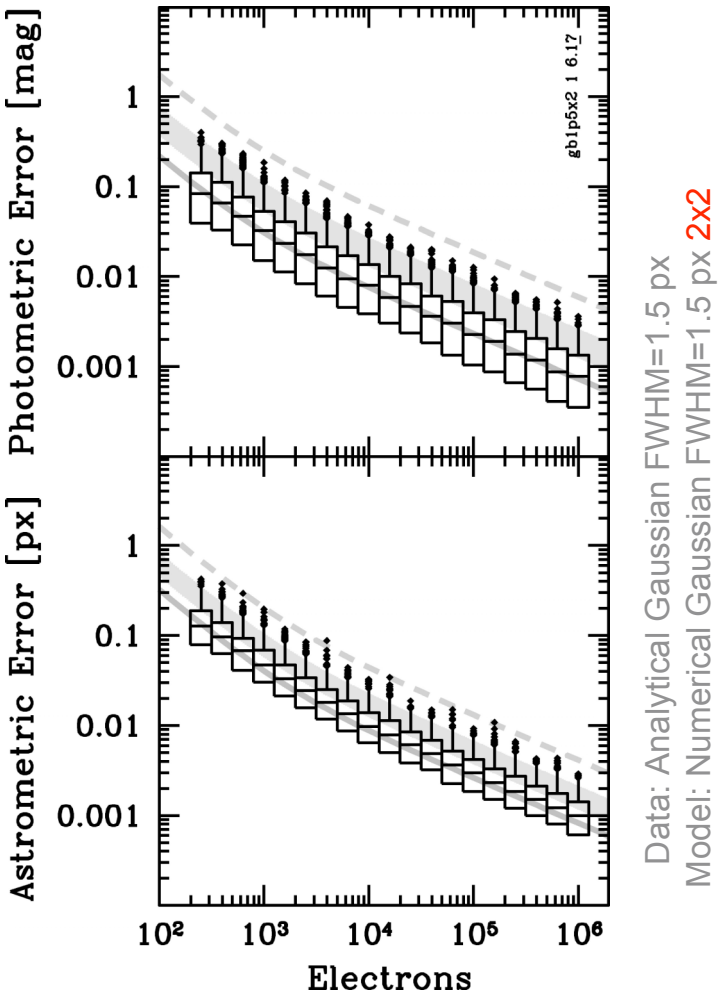


Data: Analytical Gaussian FWHM=1.5 px
Model: Numerical Gaussian FWHM=1.5 px 2x2

# Ugly (real) PSFs?

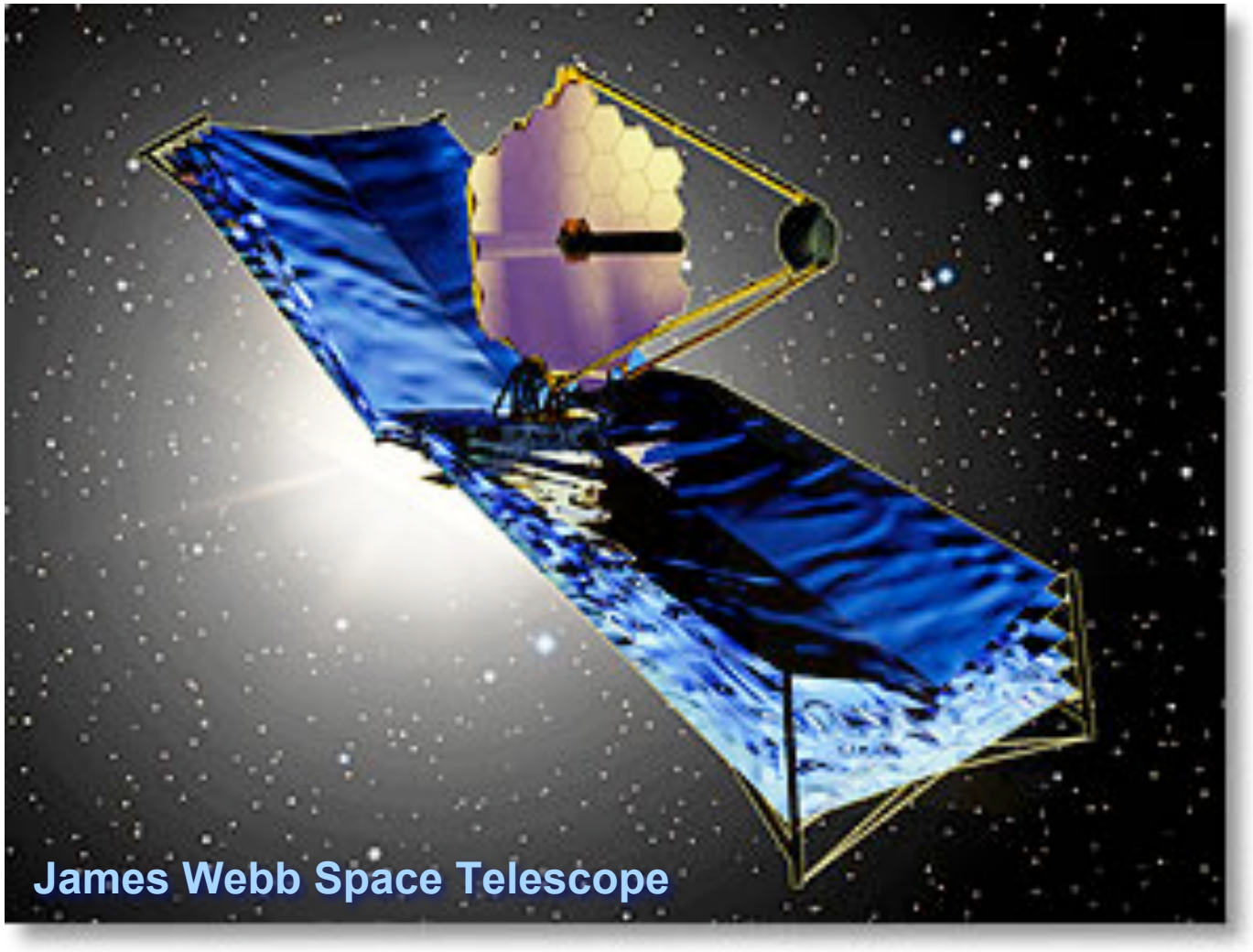

## Next Generation Space Telescope

8-m TRW-concept

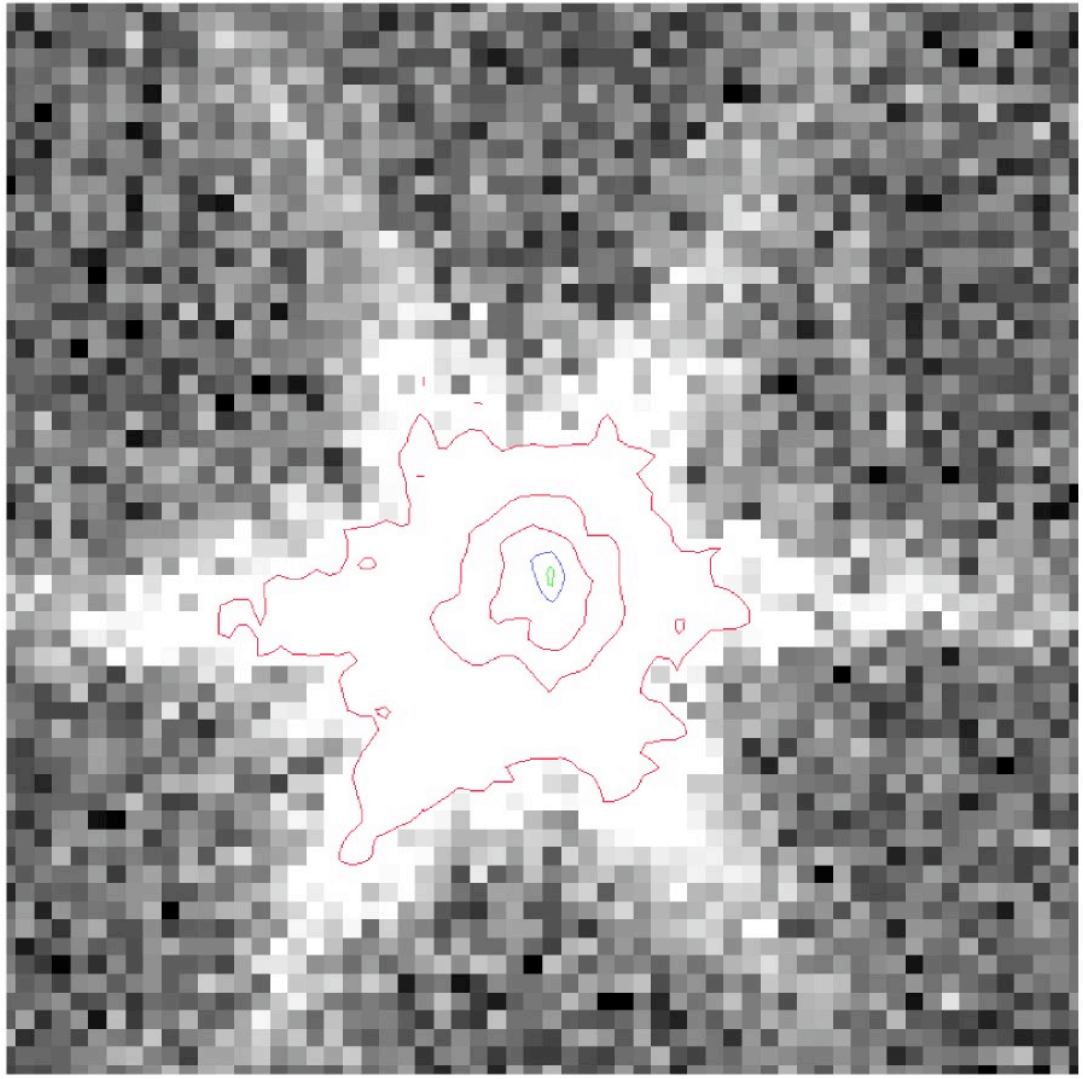

0.0128 arcsec/pixel β=31.05 PSF by John Krist

contours: 90%, 50%, 10%, 1%, 0.1% of peak

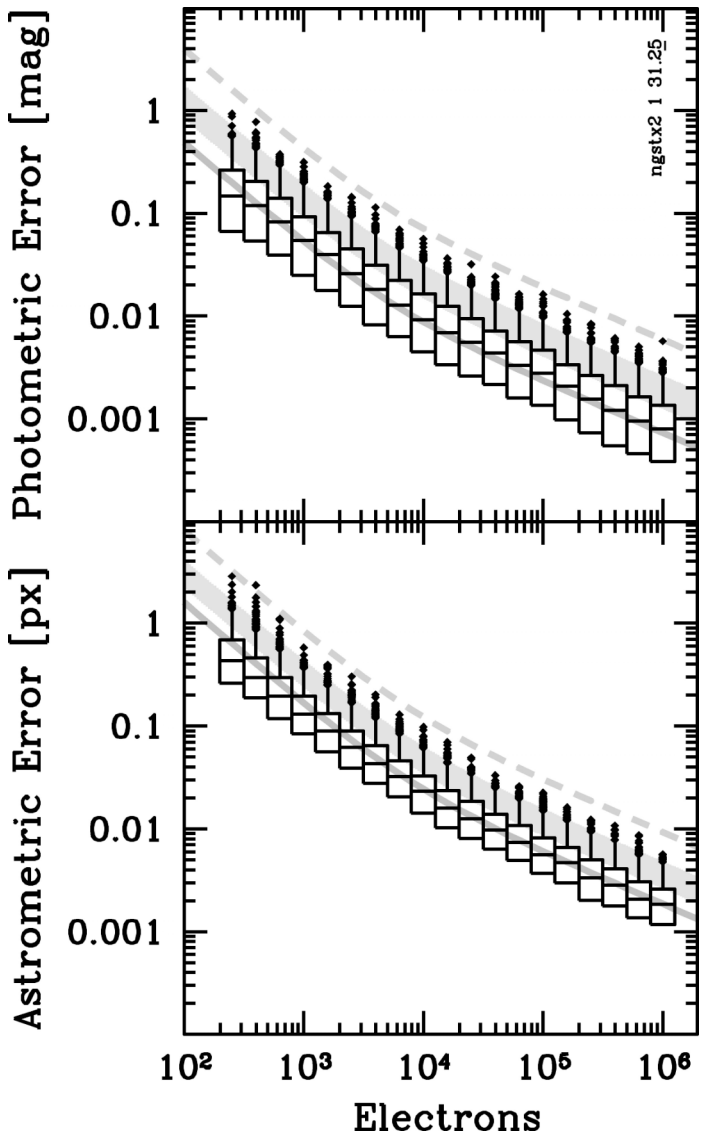
Photometric Error [mag]
Astrometric Error [px]
ngstx2 1 31.25
1
0.1
0.01
0.001
$10^2$
$10^3$
$10^4$
$10^5$
$10^6$
Electrons

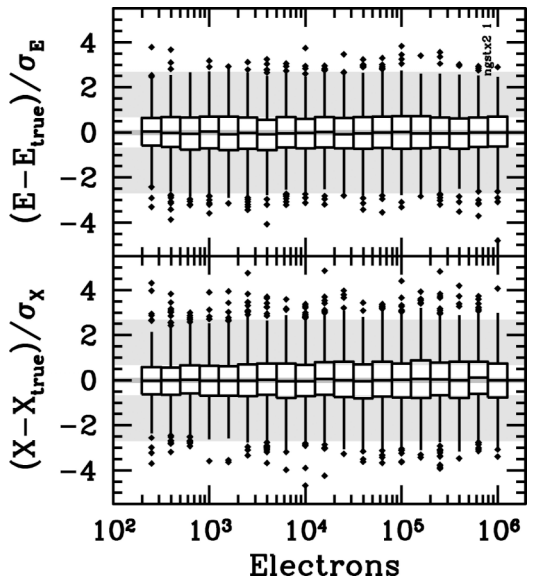
$(E-E_{true})/\sigma_E$
$(X-X_{true})/\sigma_X$
ngstx2 1
4
2
0
−2
−4
$10^2$
$10^3$
$10^4$
$10^5$
$10^6$
Electrons

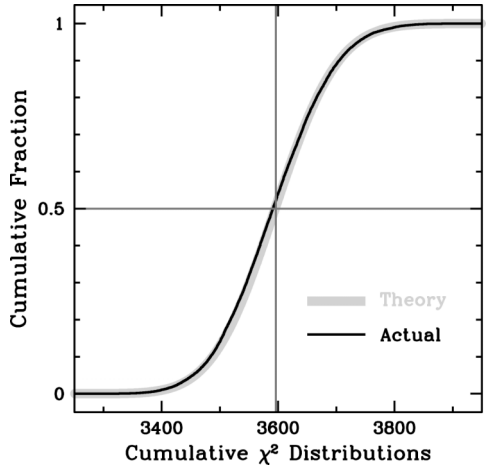
Cumulative Fraction
1
0.5
0
Theory
Actual
3400
3600
3800
Cumulative $\chi^2$ Distributions

# Calibration Errors

# Challenges of PSF Extraction

- highly variable PSF within the field of view
- too few stars
- which are not bright enough
- from undersampled observations
- that are poorly dithered
- with
  - significant Charge Transfer Efficiency variations
  - variable diffusion
  - loss of photons due to charge leakage
- and may possibly be nonlinear at <1% level

# Spitzer Space Telescope's Infrared Array Camera

Infrared Array Camera

Spitzer Space Telescope

| ID | RA_HMS | DEC_DMS | EXPTIME | DATE_OBS | DS_IDENT |
|---|---|---|---|---|---|
| 1 | 17h06m11.6s | +73d40m11s | 0.4 | 2003-10-08T11:55:51.356 | ads/sa.spitzer#0006875392 |
| 2 | 17h06m11.1s | +73d40m11s | 0.4 | 2003-10-08T12:08:56.748 | ads/sa.spitzer#0006876672 |
| 3 | 17h06m10.8s | +73d40m10s | 0.4 | 2003-10-08T12:22:01.538 | ads/sa.spitzer#0006876928 |
| 4 | 17h06m10.6s | +73d40m09s | 0.4 | 2003-10-08T12:35:06.524 | ads/sa.spitzer#0006877184 |
| 5 | 17h06m11.3s | +73d40m12s | 0.4 | 2003-10-08T12:48:11.510 | ads/sa.spitzer#0006877440 |
| 6 | 17h06m10.9s | +73d40m12s | 0.4 | 2003-10-08T13:01:16.496 | ads/sa.spitzer#0006877696 |
| 7 | 17h06m10.5s | +73d40m11s | 0.4 | 2003-10-08T13:14:21.489 | ads/sa.spitzer#0006877952 |
| 8 | 17h06m10.2s | +73d40m11s | 0.4 | 2003-10-08T13:27:26.471 | ads/sa.spitzer#0006878208 |
| 9 | 17h06m11.0s | +73d40m14s | 0.4 | 2003-10-08T13:40:31.472 | ads/sa.spitzer#0006878464 |
| 10 | 17h06m10.7s | +73d40m13s | 0.4 | 2003-10-08T13:53:36.446 | ads/sa.spitzer#0006878720 |
| 11 | 17h06m10.5s | +73d40m13s | 0.4 | 2003-10-08T14:06:41.436 | ads/sa.spitzer#0006878976 |
| 12 | 17h06m10.0s | +73d40m12s | 0.4 | 2003-10-08T14:19:46.422 | ads/sa.spitzer#0006879232 |
| 13 | 17h06m11.0s | +73d40m15s | 0.4 | 2003-10-08T14:32:51.423 | ads/sa.spitzer#0006879488 |
| 14 | 17h06m10.5s | +73d40m15s | 0.4 | 2003-10-08T15:06:39.788 | ads/sa.spitzer#0006879744 |
| 15 | 17h06m10.3s | +73d40m14s | 0.4 | 2003-10-08T15:19:44.785 | ads/sa.spitzer#0006880000 |
| 16 | 17h06m10.0s | +73d40m13s | 0.4 | 2003-10-08T15:32:49.763 | ads/sa.spitzer#0006880256 |

typical observation

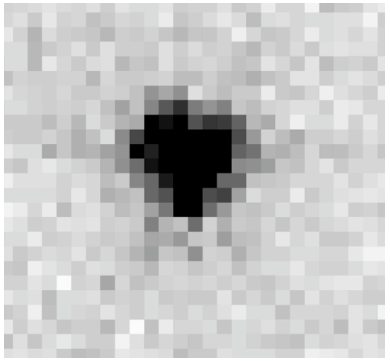

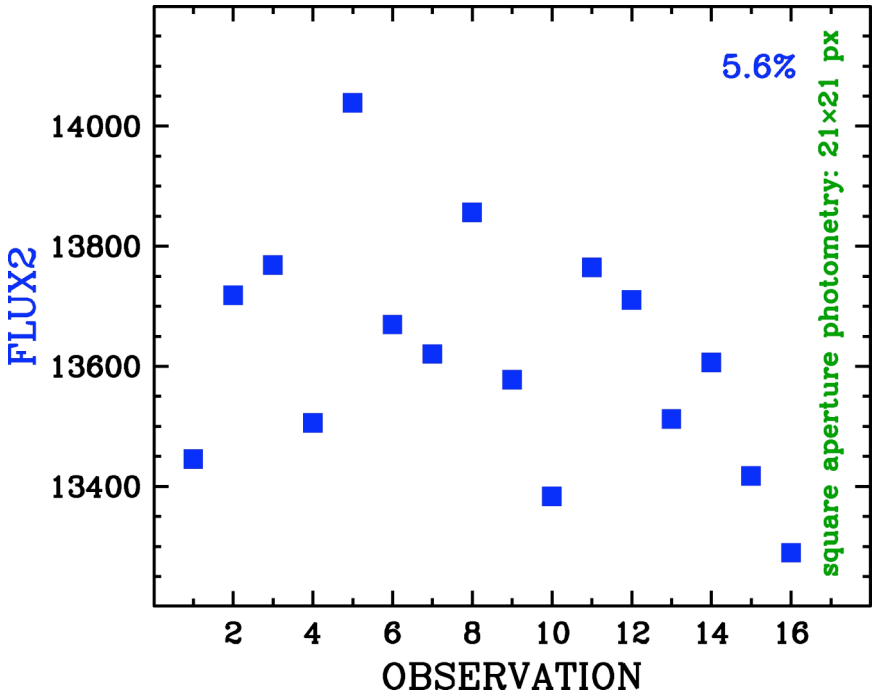


A 5.6% peak-to-peak range in measured flux values within a 21x21 pixel square aperture.

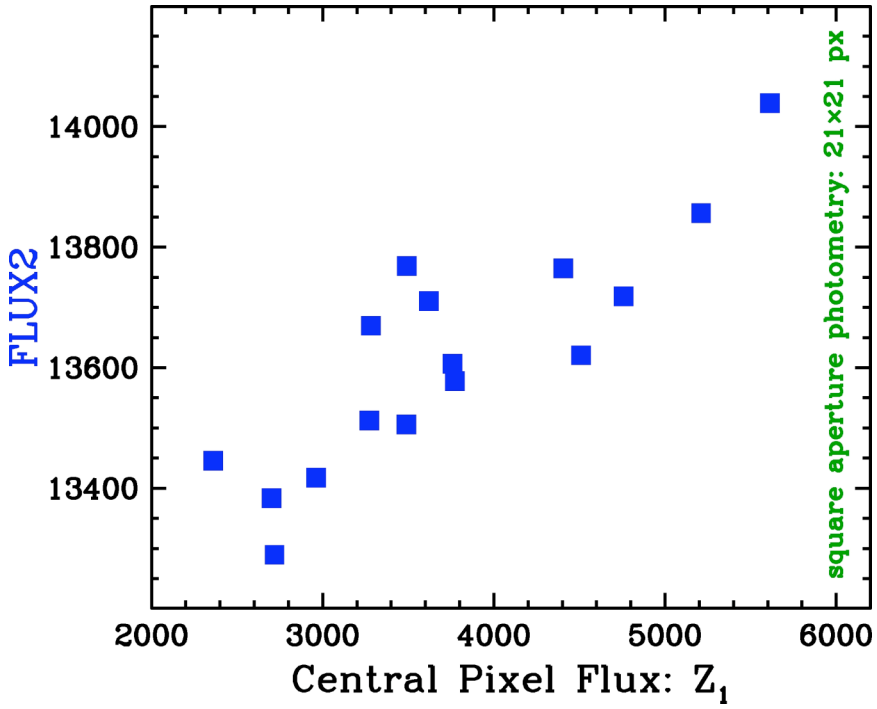


Not all of the variation is random!

Stars centered in the middle of a pixel have more flux than those that are centered on a pixel corner.

# IRAC Data Handbook

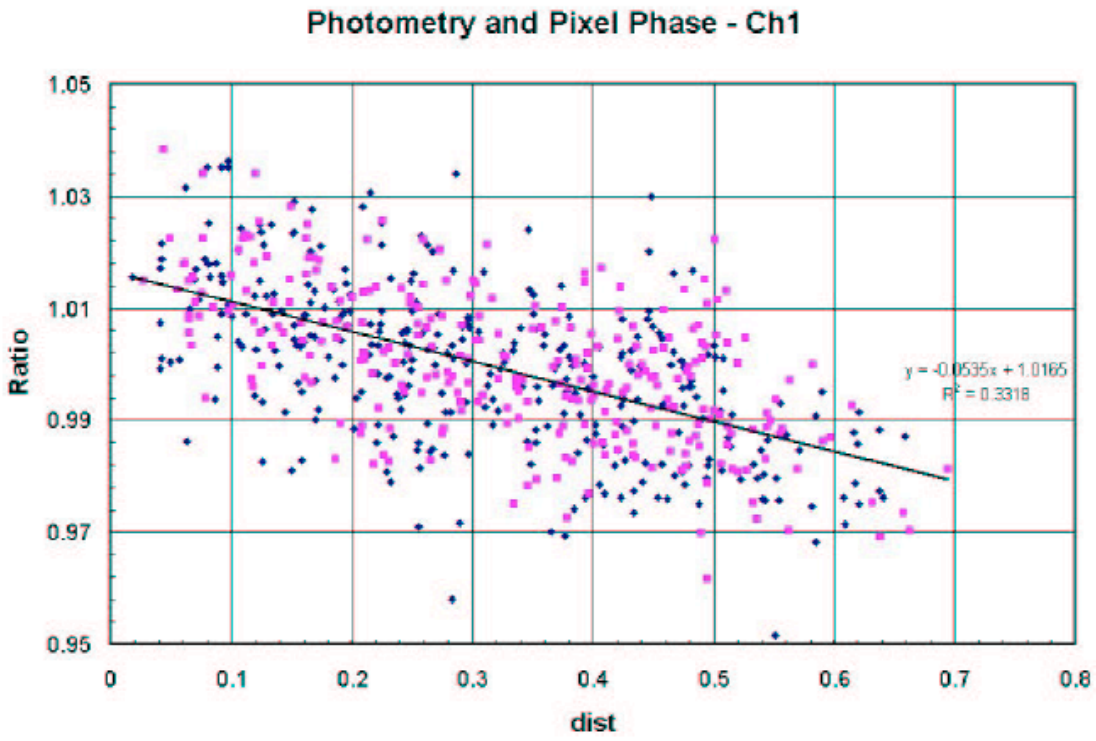


Figure 5.1: Dependence of point source photometry on the distance of the centroid of a point source from the nearest pixel center in channel 1. The ratio on the vertical axis is the measured flux density to the mean value for the star, and the quantity on the horizontal axis is the fractional distance of the centroid from the nearest pixel center.

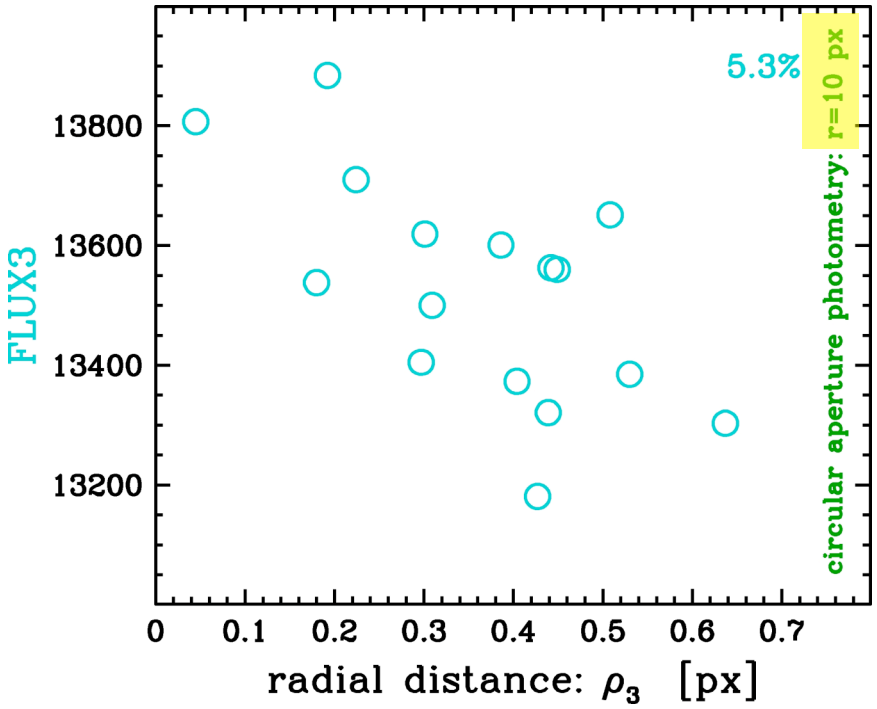


A 5.3% peak-to-peak range in measured flux values within an aperture radius of 10 pixels.

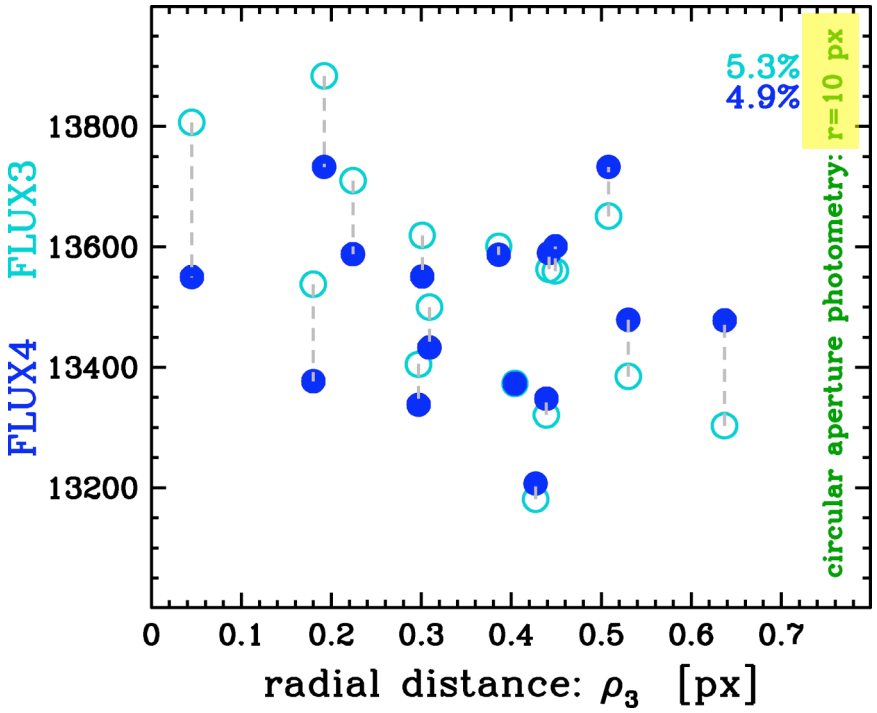


uncorrected
corrected

A 4.9% peak-to-peak range using the recommended radial correction.

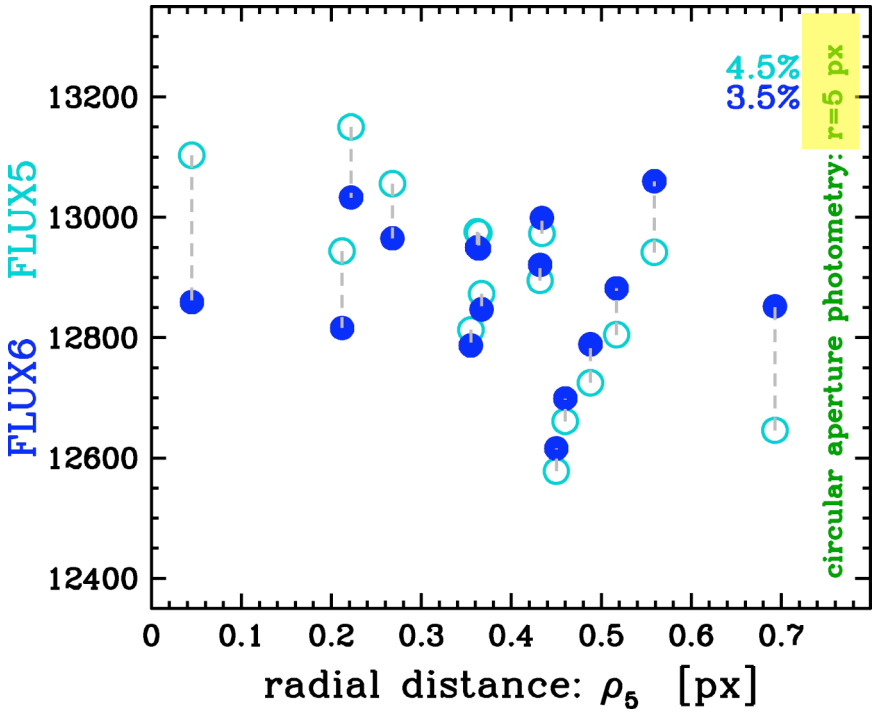


uncorrected
corrected

A 3.5% peak-to-peak range in measured flux values within an *aperture radius of 5 pixels* and using the recommended radial correction.

# IRAC Ch1 PSF (5x5 theoretical)

linear stretch

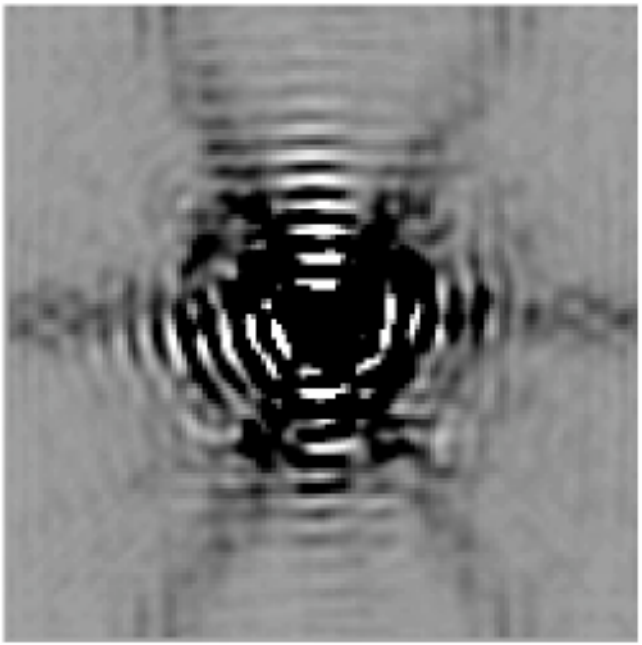

logarithmic stretch

Source: Bill Hoffmann
(U. of Arizona, IRAC team member)

# Relative Intrapixel QE Variation of IRAC Ch1

$$\text{intrapix} = \begin{pmatrix} 0.813 & 0.875 & 0.875 & 0.875 & 0.813 \\ 0.875 & 1.000 & 1.000 & 1.000 & 0.875 \\ 0.875 & 1.000 & 1.000 & 1.000 & 0.875 \\ 0.875 & 1.000 & 1.000 & 1.000 & 0.875 \\ 0.813 & 0.875 & 0.875 & 0.875 & 0.813 \end{pmatrix}$$

Source: Bill Hoffmann
(U. of Arizona, IRAC team member)

# Lost flux can be recovered

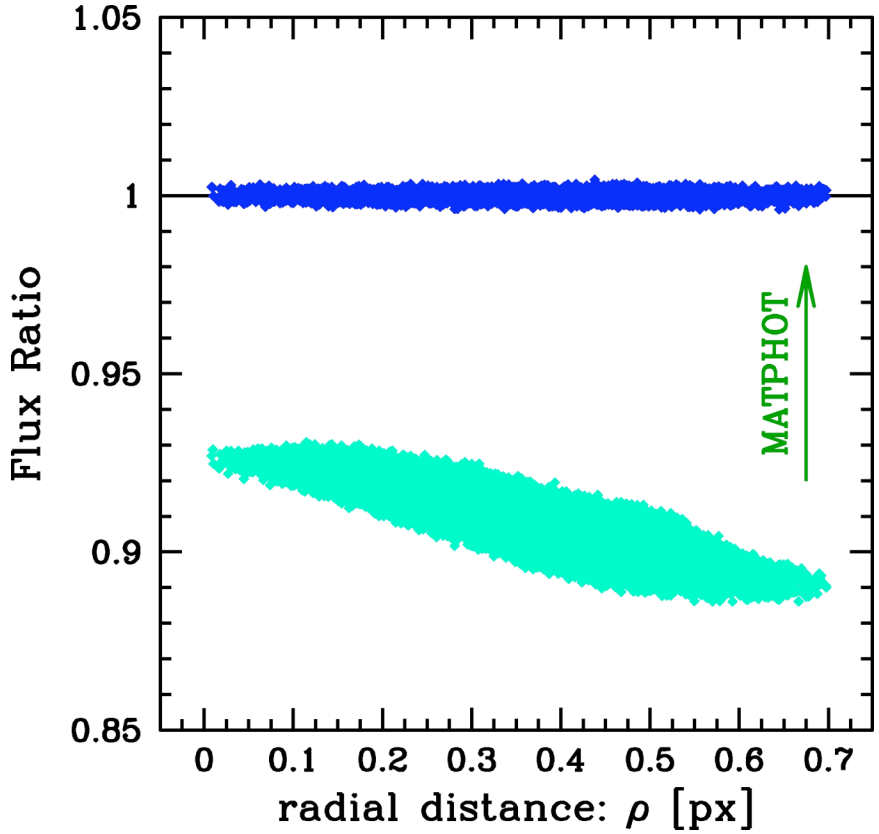


◀ random errors

◀ ***systematic*** errors

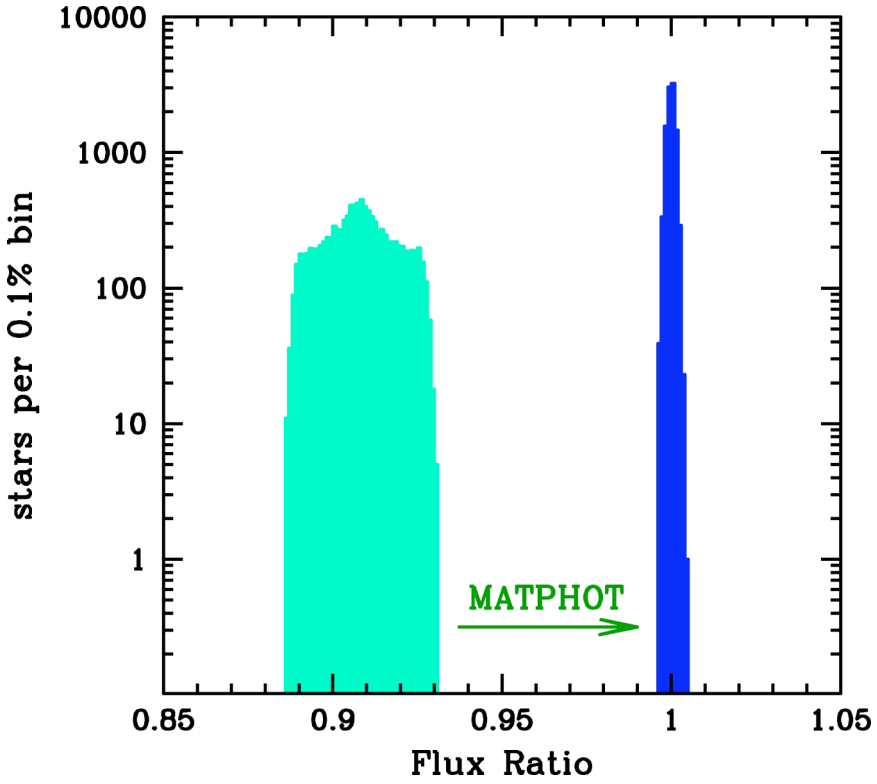
10000
1000
100
10
1
stars per 0.1% bin
MATPHOT
0.85
0.9
0.95
1
1.05
Flux Ratio

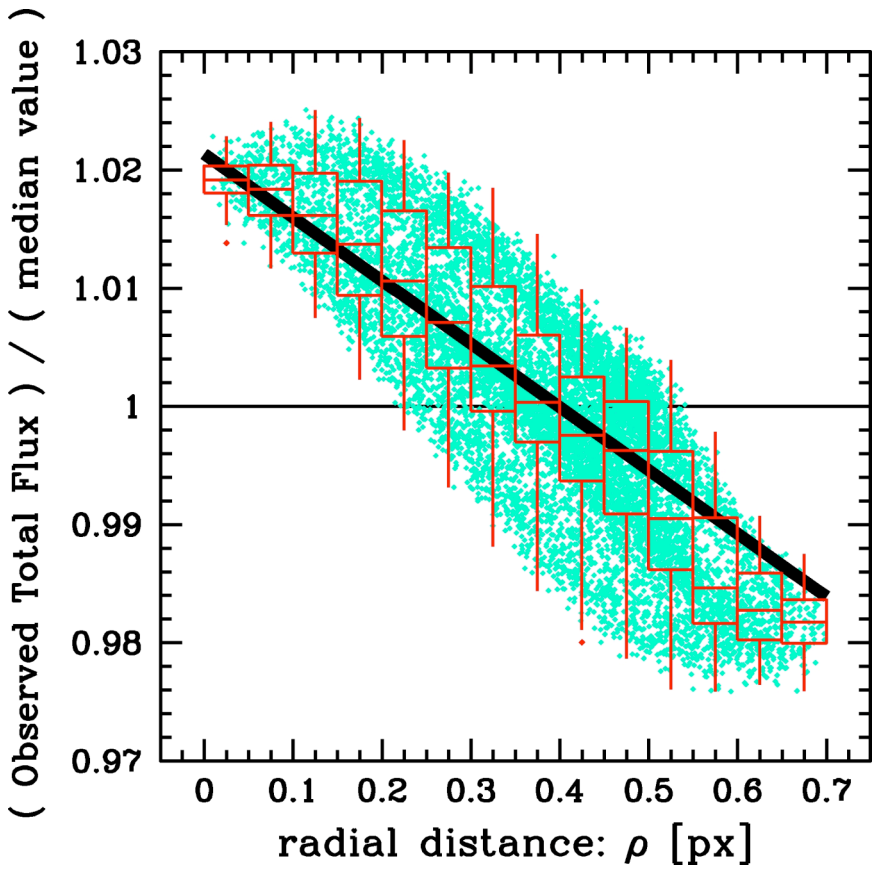


The recommended radial correction may leave a significant systematic error of a few percent.

# MATPHOT Photometry

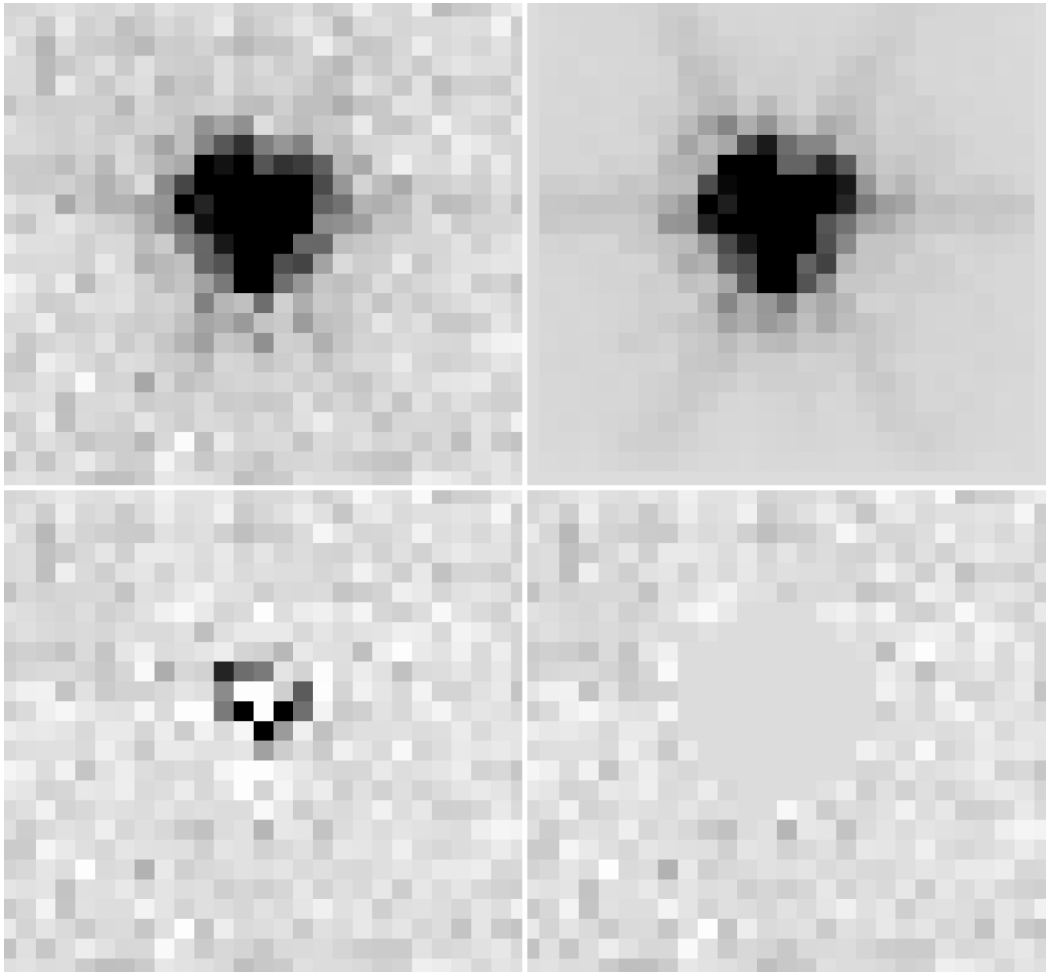

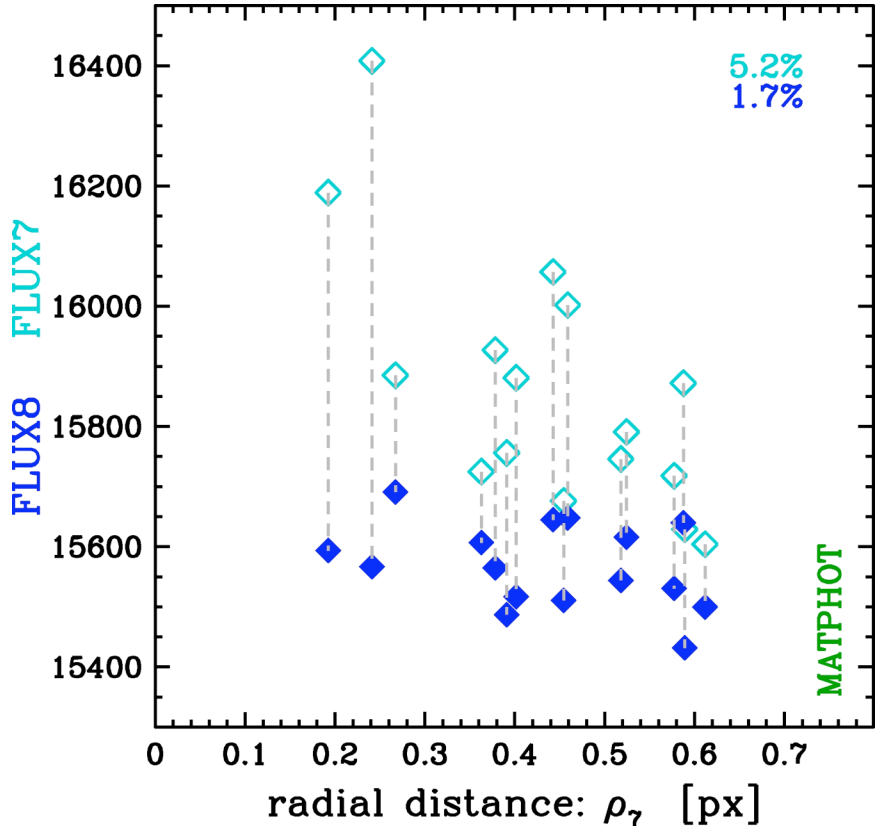


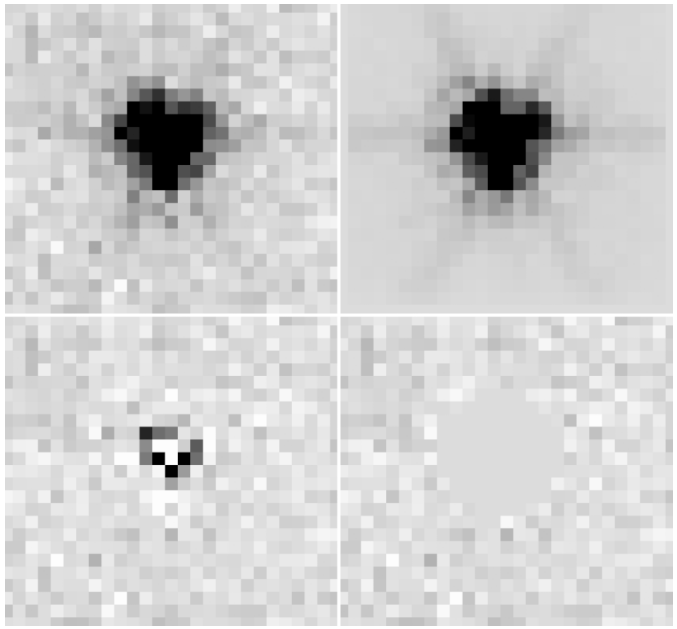

MATPHOT
with residuals

A 1.7% peak-to-peak range using MATPHOT flux measurements *with residuals within 5 pixels*.

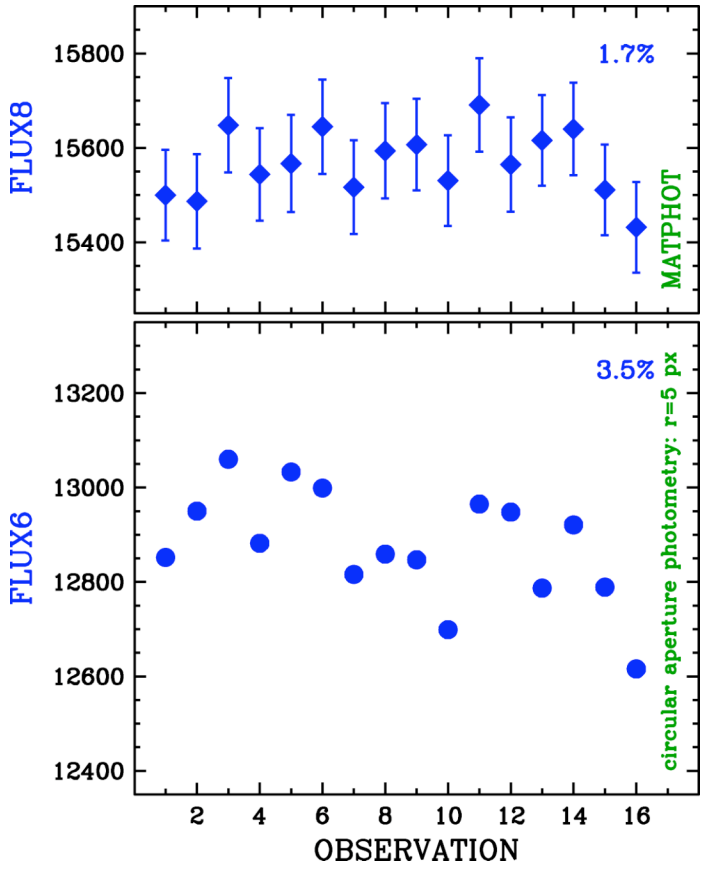


An improvement of 100% over the best results from aperture photometry using MATPHOT with residuals.

| ID | $X_7$ | $Y_7$ | FLUX7 | FLUX8 | $B_7$ | $\rho_7$ | VOLUME | NOISEPX |
|---|---|---|---|---|---|---|---|---|
| 1 | 132.529 | 125.391 | $15604 \pm 96$ | 15500 | 0.031 | 0.6118 | 0.889241 | 9.849 |
| 2 | 132.383 | 127.081 | $15756 \pm 100$ | 15487 | 0.062 | 0.3912 | 0.911503 | 6.357 |
| 3 | 132.277 | 128.366 | $16002 \pm 100$ | 15648 | 0.065 | 0.4589 | 0.901929 | 7.863 |
| 4 | 132.448 | 129.260 | $15746 \pm 98$ | 15544 | 0.088 | 0.5181 | 0.896910 | 8.521 |
| 5 | 131.197 | 125.860 | $16408 \pm 103$ | 15567 | 0.140 | 0.2412 | 0.925153 | 4.755 |
| 6 | 131.026 | 127.442 | $16057 \pm 100$ | 15645 | 0.096 | 0.4426 | 0.905820 | 7.435 |
| 7 | 130.971 | 128.599 | $15881 \pm 99$ | 15517 | 0.086 | 0.4017 | 0.910432 | 6.489 |
| 8 | 130.866 | 129.862 | $16189 \pm 101$ | 15594 | 0.092 | 0.1925 | 0.919395 | 5.478 |
| 9 | 129.737 | 126.250 | $15725 \pm 97$ | 15607 | 0.136 | 0.3629 | 0.898101 | 8.424 |
| 10 | 129.669 | 127.473 | $15718 \pm 96$ | 15531 | 0.146 | 0.5774 | 0.889749 | 9.571 |
| 11 | 129.795 | 128.172 | $15885 \pm 99$ | 15691 | 0.170 | 0.2673 | 0.906094 | 7.173 |
| 12 | 129.623 | 129.971 | $15927 \pm 100$ | 15565 | 0.174 | 0.3783 | 0.908991 | 7.253 |
| 13 | 128.649 | 125.610 | $15791 \pm 96$ | 15616 | 0.123 | 0.5244 | 0.895622 | 8.549 |
| 14 | 128.370 | 127.543 | $15872 \pm 98$ | 15640 | 0.078 | 0.5876 | 0.898904 | 7.922 |
| 15 | 128.627 | 128.259 | $15676 \pm 96$ | 15511 | 0.112 | 0.4544 | 0.894073 | 9.229 |
| 16 | 128.664 | 129.484 | $15629 \pm 96$ | 15432 | 0.102 | 0.5893 | 0.889795 | 9.532 |

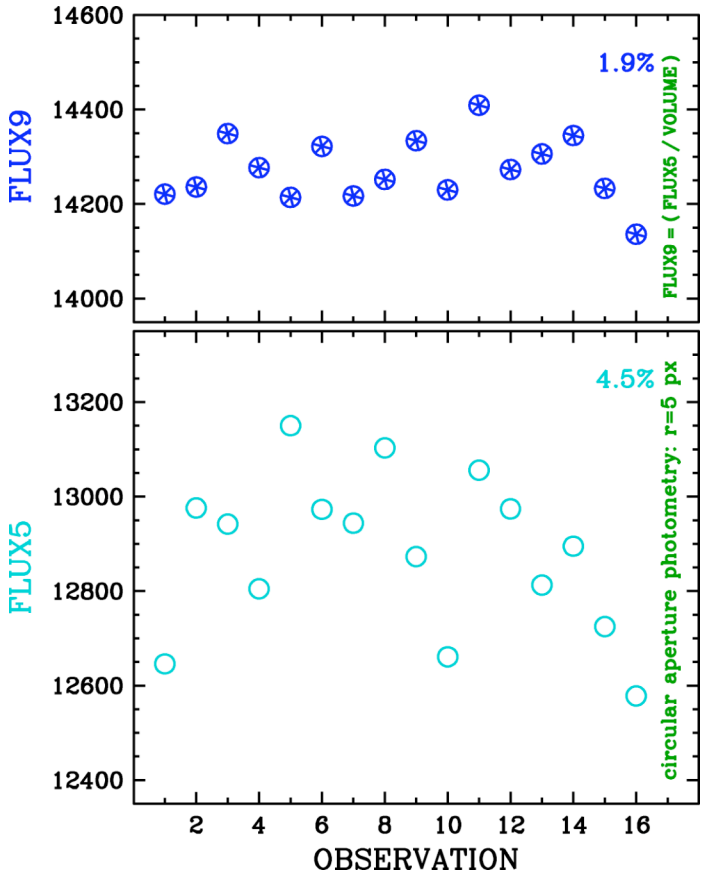


corrected
uncorrected

An improvement of >100% for *aperture photometry* corrected with MATPHOT computed PRF volumes.

This work is supported by a grant, Interagency Order No. NNG06EC81I, from the **Applied Information Systems Research (AISR)** Program of the Science Mission Directorate of the National Aeronautics and Space Administration (NASA).